

RESEARCH TECHNICAL REPORT

*Numerical Simulations of
Sprinkler Activations and
Spray Transport under
Obstructed, Sloped Ceilings*



Numerical Simulations of Sprinkler Activations and Spray Transport under Obstructed, Sloped Ceilings

Prepared by

Prateep Chatterjee¹ and Justin A. Geiman²

¹ FM Global, Research Division, 1151 Boston-Providence Turnpike, Norwood, MA 02062

² Fire and Risk Alliance, 7640 Standish Place, Rockville, MD 20855

September 2017

PROJECT ID 0003059743

Disclaimer

The research presented in this report, including any findings and conclusions, is for informational purposes only. Any references to specific products, manufacturers, or contractors do not constitute a recommendation, evaluation or endorsement by Factory Mutual Insurance Company (FM Global) of such products, manufacturers or contractors. FM Global does not address life, safety, or health issues. The recipient of this report must make the decision whether to take any action. FM Global undertakes no duty to any party by providing this report or performing the activities on which it is based. FM Global makes no warranty, express or implied, with respect to any product or process referenced in this report. FM Global assumes no liability by or through the use of any information in this report.

Executive Summary

In conjunction with the Property Insurance Research Group (PIRG) and in collaboration with the Fire Protection Research Foundation (FPRF), the research affiliate of the National Fire Protection Association (NFPA), this study investigates the impact of sloped ceilings with obstructed construction on fire protection requirements. The current study is aligned with the FPRF "Protection of Storage Under Sloped Ceilings – Phase 2" project. The goal of this project is to support the NFPA 13 Technical Committee and FM Global standards in the development of new protection requirements addressing sprinkler installation beneath sloped ceilings. Phase 2 of the project extends the parameter space covered in Phase 1 of the project [i], namely the inclusion of obstructed ceiling construction (e.g., purlins and girders), ridges and analysis of additional sprinkler types.

The aim of the study is to provide guidance to the sprinkler installation standards and the large-scale tests planned in Phase 3 of the FPRF project by conducting the following:

- Evaluate sprinkler activation times and patterns from large-scale growing fires in the presence of obstructed ceiling construction, ridges and over a range of slopes.
- Evaluate the effect of ceiling inclination on water-flux distributions over a rack-storage commodity for upright and pendent type sprinklers.
- Understand the effect of sprinklers oriented with the deflector parallel to the ceiling or to the floor.

To meet this aim, a modeling-based investigation has been conducted using the computational fluid dynamics (CFD) code FireFOAM [ii][iii]. The numerical modeling work was performed by FM Global in collaboration with Fire and Risk Alliance [iv], the FPRF contractor. The modeling work has been divided into two parts: 1) a sprinkler-activation study, and 2) a sprinkler-spray investigation, as described below.

1. For sprinkler activation predictions, simulations were performed of ceiling jets resulting from a growing fire on a 3-tier-high rack-storage array of Cartoned Unexpanded Plastic (CUP) commodity. Ceiling clearances of 3.05 m (10 ft) and 6.1 m (20 ft) were selected and ceiling inclinations between 0° and 18.4° have been considered. Obstructed ceiling construction features in the form of purlins and girders were included in the simulations. Purlin depths of 0.1-0.6 m (4-24 in.) and a girder depth of 0.6 m (24 in.) were considered. Purlins and girders were separated by distances of 1.5 m (5 ft) and 7.6 m (25 ft), respectively. The ranges for ceiling

[i] P. Chatterjee and K. V. Meredith, "Numerical Modeling of Sprinkler Activations and Spray Transport Under Sloped Ceilings," FM Global, Technical Report 2015.

[ii] FireFOAM: available from <http://www.fmglobal.com/modeling>

[iii] Y. Wang, P. Chatterjee, and J. L. de Ris, "Large Eddy Simulation of Fire Plumes," *Proceedings of the Combustion Institute*, vol. 33, no. 2, pp. 2473-2480, 2011.

[iv] Fire and Risk Alliance, <http://www.fireriskalliance.com>

clearance, inclination and obstruction depths were selected based on conclusions from the Phase 1 study [i] and considering prevailing storage conditions in the industry [v]. Sprinkler activation simulations were also conducted with a ceiling containing a symmetrical ridge with obstructed ceiling construction. The distance between the center of the commodity and the ridge was kept at 6.1 and 12.2 m (20 and 40 ft), measured along the slope of the ceiling.

2. The effects of slope and deflector orientation on sprinkler spray were also investigated for smooth ceilings. An upright K160 lpm/bar^{0.5} (K11.2 gpm/psi^{0.5}) and a pendent K240 lpm/bar^{0.5} (K16.8 gpm/psi^{0.5}) sprinkler were selected in addition to the K200 lpm/ bar^{0.5} (K14.0 gpm/ psi^{0.5}) studied in Phase 1. The water-flux distribution reaching the top of the rack-storage array was simulated. The water-flux estimations have been made for the ignition location under one sprinkler as well as among four sprinklers. For the spray simulations, obstructed ceiling construction aspects have not been included since FM Global [vi] and NFPA [vii] installation standards ensure sprinkler locations are adjusted to eliminate spray obstructions caused by ceiling structural elements.

Ceiling inclination causes biased flow of the fire plume toward the elevated ceiling side due to buoyancy effects. However, the presence of purlins affects the upward flow pattern and tends to provide confinement of the combustion products. Results show that increasing purlin depth for a given ceiling inclination generally causes greater skewness of the activation pattern in the direction of the purlin channels.

From activation simulations, the following specific conclusions are drawn for quick-response, ordinary temperature (QR/OT) sprinklers, based on the four sprinklers immediately adjacent to the fire source:

- For horizontal ceilings (0°) and purlin depths of up to 0.6 m (24 in.), a marginal increase (maximum 4 s) in the average activation time is observed.
- For a ceiling inclination of 9.5° and purlin depths of up to 0.3 m (12 in.), the average activation times are similar as in the case of horizontal ceilings for the same purlin depths. The average activation times are also comparable to those of the 9.5° smooth ceiling. For a purlin depth of 0.6 m (24 in.), considerable activation delay is observed for the non-elevated sprinklers. This delay may adversely impact suppression performance.
- For a ceiling inclination of 18.4° and purlin depths of up to 0.1 m (4 in.), the average activation time compares favorably with the smooth ceiling results. For the same slope and purlin depths of 0.2 m (8 in.) and larger, considerable delays in non-elevated sprinkler activations are also observed which may affect suppression effectiveness.

[v] K. E. Isman, S. J. Jordan, A. W. Marshall, and N. L. Ryder, "Research Plan for Sloped Ceiling Storage Protection," *Fire Protection Research Foundation Report*, November 2015.

[vi] FM Global Data Sheet 2-0: *Installation Guidelines for Automatic Sprinklers*. January 2014.

[vii] NFPA 13: *Standard for the Installation of Sprinkler Systems*. 2016.

- The presence of ridges marginally affects the activation times of the four sprinklers surrounding the ignition location. Activations near the ridge are also affected with slightly earlier activation times observed on the near side of the ridge.

For standard-response, high temperature (SR/HT) sprinklers, the following conclusions can be drawn:

- For SR/HT sprinklers, for ceilings 3.05 m (10 ft) above the CUP array and at inclination angles $\geq 9.5^\circ$ with a purlin depth of 0.3 m (12 in.), highly skewed activation patterns are observed between the elevated and non-elevated sides. As sprinklers on the non-elevated side do not activate, suppression effectiveness is reduced.
- For an inclined ceiling at 18.4° with the ridge located 6.1 m (20 ft) from the CUP array, activation times near the ignition region are similar to those observed when the ridge is not present; however, significantly more SR/HT sprinklers activate near the ridge compared to an unbounded ceiling. The effect of the ceiling ridge on the sprinkler activation patterns appears to be more significant for SR/HT than for QR/OT sprinklers.

For sprinkler spray considerations, the following conclusions can be drawn:

- For a single sprinkler above the ignition location when the fire plume is not present, for both the upright K160 and pendent K240 sprinklers, increasing the ceiling inclination from 0° to 18.4° causes a slight decrease in the water flux to the top of the rack-storage array, and the deflector orientation has negligible effect on the water-flux distribution.
- For one upright K160 sprinkler directly above a 600-kW fire, the water-flux distribution is reduced significantly above the ignition location when the deflector is held parallel-to-ceiling. The same observation also holds true for the pendent K240 sprinkler.
- For ignition among four sprinklers, in the presence of a 2.6-MW fire plume, the performance of the upright K160 sprinkler remains similar, irrespective of the deflector orientation. For the pendent K240 sprinkler, a small decrease in mass flow rate is observed when the deflector parallel-to-ceiling orientation is selected. Results confirm the conclusions from a study conducted earlier that the sprinkler deflector parallel-to-floor is a preferable orientation.

Based on the conclusions detailed above and from the Phase 1 study [i] a large-scale test plan can now be developed. The large-scale tests will provide validation of the simulation results. Test and modeling results will be used to update FM Global and NFPA standards [vi] [vii].

Abstract

In the present study, an investigation based on numerical modeling was conducted to facilitate understanding of protection challenges associated with sloped ceilings. The modeling study was conducted using the computational fluid dynamics (CFD) code FireFOAM. Ceiling jets resulting from growing fires on a 3-tier-high CUP rack-storage commodity were simulated to investigate the effect of obstructed ceiling construction (purlins and girders) and the presence of ridges on sprinkler activations below inclined ceilings. For quick-response, ordinary temperature sprinklers, simulation results show that, for the fire source being evaluated, ceilings up to and including 18.4° inclination with purlin depths of <0.2 m (8 in.), have similar activation times and patterns as horizontal, smooth ceilings for the four sprinklers immediately adjacent to the fire source. For smooth ceilings, the presence of a ridge at a 6.1 m (20 ft) distance from the ceiling mid-point caused marginal activation delays for the four sprinklers surrounding the ignition location. In presence of purlins, the ridge caused considerable reduction of activation times. Spray transport simulations were also conducted to evaluate the effect of ceiling slope and sprinkler installation orientations on water-flux distributions for an upright K160 sprinkler and a pendent K240 sprinkler. Results confirm the conclusions from a study conducted earlier that the sprinkler deflector parallel-to-floor is a preferable orientation.

Acknowledgments

The authors wish to thank Dr. Karl Meredith for providing the sprinkler injection models and for his considerable editorial input. The authors would also like to thank Dr. Yi Wang for providing key technical feedback on several occasions. Ms. Amanda Kimball of the NFPA FPRF is recognized and appreciated for ensuring the project stayed on track and for organizing regular progress meetings. Feedback throughout the project duration was received from Drs. André Marshall, Ankur Gupta, Francesco Tamanini, Sergey Dorofeev, and Messrs. Weston Baker and Noah Ryder. Their contributions are gratefully acknowledged. Dr. Louis Gritzo is acknowledged for his continued support toward the successful completion of the project. The NFPA FPRF technical panel members are also thanked for providing their feedback.

Table of Contents

Executive Summary.....	i
Abstract.....	iv
Acknowledgments.....	v
Table of Contents.....	vi
List of Figures	viii
List of Tables	xi
1. Introduction	1
1.1 Objectives.....	3
1.2 Technical Approach.....	3
2. Numerical Model	8
2.1 FireFOAM Solver	8
2.2 Mesh Generation	8
2.3 Fire Growth Model.....	9
2.4 Sprinkler Activation Setup.....	11
2.5 Sprinkler Spray Setup	11
3. Sprinkler Activation Study.....	12
3.1 Ceiling Flows in Presence of Obstructed Construction.....	12
3.1.1 Ceiling Jet Development	12
3.1.1 Activations of Quick-Response, Ordinary Temperature Sprinklers	13
3.1.1.1 Horizontal Ceiling.....	16
3.1.1.2 Inclined Ceiling (9.5°).....	17
3.1.1.3 Inclined Ceiling (18.4°).....	20
3.1.1.4 Comparison with Smooth Ceiling Activation Times.....	20
3.1.2 Activations of Standard-Response, High Temperature Sprinklers.....	21
3.1.3 Effect of Ceiling Clearance	22
3.2 Ceiling Flows in the Presence of Ridges.....	22
3.2.1 Ceiling Jet Development	22
3.2.2 Activation of Quick-Response, Ordinary Temperature Sprinklers.....	24
3.2.2.1 Inclined Ceiling (9.5°).....	25
3.2.2.2 Inclined Ceiling (18.4°).....	26
3.2.2.3 Comparison of Smooth, Inclined Ceiling Activation Times.....	27
3.2.3 Activations of Standard-Response, High Temperature Sprinklers.....	28

3.3	Summary	29
4.	Sprinkler Sprays Study	31
4.1	Sprinkler Operating Conditions and Ceiling Inclination Selection	32
4.2	Selection of Heat Release Rates.....	32
4.3	Upright K160 Sprinkler	32
4.3.1	Water-flux Distributions from One Sprinkler.....	32
4.3.2	Comparison of Integrated Mass Flux	34
4.3.3	Water-flux Distributions from Four Sprinklers	37
4.3.4	Comparison of Integrated Mass Flux	40
4.4	Pendent K240 Sprinkler	40
4.4.1	Water-flux Distributions from One Sprinkler.....	40
4.4.2	Comparison of Integrated Mass Flux	43
4.4.3	Water-flux Distributions from Four Sprinklers	45
4.4.4	Comparison of Integrated Mass Flux	47
4.5	Summary	48
5.	Conclusions and Recommendations.....	49
	References	51

List of Figures

1-1: Obstructed ceiling construction present below a sloped ceiling: (a) purlins connected to the ceiling and a girder present along the ceiling slope, and (b) two types of purlin shapes (C- and Z-type) are shown connected to a girder.....	2
1-2: Computational setup (not to scale) showing the 3-tier-high rack-storage array: (a) front view showing purlins, girders and sprinklers below the ceilings (horizontal and inclined at θ angle), and (b) side view showing purlins and girders present below the horizontal ceiling.....	5
1-3: Computational setup (not to scale) showing a front view of the 3-tier-high rack-storage array with an inclined ceiling containing a ridge, purlins, girders and sprinklers below the ceiling.....	6
2-1: Computational mesh showing a ceiling inclined at 18.4° with its midpoint located 3.05 m (10 ft) above the rack-storage array. Purlins of a depth of 0.2 m (8 in.) are present below the ceiling.	9
2-2: Fire impinging on a ceiling with 0.2 m (8 in.) purlins and 0.6 m (24 in.) girders present. The ceiling is inclined at 18.4°	10
2-3: Modeled HRR (chemical and convective) and radiant fraction variation in time for the 2 x 2 x 3 array of CUP commodity.	10
3-1: Computed CO_2 mass fraction contours colored by temperature below a 24 m x 24 m (80 ft x 80 ft) smooth ceiling inclined at 18.4° located 3.05 m (10 ft) above the CUP array. Approximate convective HRR at the selected times are also shown.....	13
3-2: Computed CO_2 mass fraction contours colored by temperature below a 24 m x 24 m (80 ft x 80 ft) ceiling inclined at 18.4° with 0.1 m (4 in.) deep purlins located 3.05 m (10 ft) above the CUP array.	14
3-3: Computed CO_2 mass fraction contours colored by temperature below a 24 m x 24 m (80 ft x 80 ft) ceiling inclined at 18.4° with 0.2 m (8 in.) deep purlins located 3.05 m (10 ft) above the CUP array.	14
3-4: Computed CO_2 mass fraction contours colored by temperature below a 24 m x 24 m (80 ft x 80 ft) ceiling inclined at 18.4° with 0.3 m (12 in.) deep purlins located 3.05 m (10 ft) above the CUP array.	15
3-5: Computed CO_2 mass fraction contours colored by temperature below a 24 m x 24 m (80 ft x 80 ft) ceiling inclined at 18.4° with 0.6 m (24 in.) deep purlins located 3.05 m (10 ft) above the CUP array.	15
3-6: Activation of QR/OT sprinklers located 0.33 m (13 in.) below a horizontal ceiling 3.05 m (10 ft) above the CUP array when purlin depth is (a) 0.1 m (4 in.), (b) 0.2 m (8 in.), (c) 0.3 m (12 in.), and (d) 0.6 m (24 in.). Purlins and girders are overlaid on top of the contours. Ceiling is 24 m x 24 m (80 ft x 80 ft).....	16
3-7: Activation of QR/OT sprinklers located 0.33 m (13 in.) below a ceiling inclined at 9.5° with its midpoint 3.05 m (10 ft) above the CUP array when purlin depth is (a) 0.1 m (4 in.), (b) 0.2 m (8 in.), (c) 0.3 m (12 in.), and (d) 0.6 m (24 in.). Purlins and girders are overlaid on top of the contours.	18

3-8: Activation of QR/OT sprinklers located 0.33 m (13 in.) below a ceiling inclined at 18.4° with its midpoint 3.05 m (10 ft) above the CUP array when purlin depth is (a) 0.1 m (4 in.), (b) 0.2 m (8 in.), (c) 0.3 m (12 in.), and (d) 0.6 m (24 in.). Purlins and girders are overlaid on top of the contours.	19
3-9: Activation of SR/HT sprinklers located 0.33 m (13 in.) below ceilings with their midpoints 3.05 m (10 ft) above the CUP array when purlin depth is 0.3 m (12 in.). Ceiling inclinations are (a) 9.5°, and (b) 18.4°. Purlins and girders are overlaid on top of the contours.	21
3-10: Activation of QR/OT sprinklers located 0.33 m (13 in.) below a ceiling inclined at 18.4° with its midpoint 6.1 m (20 ft) above the CUP array when purlin depth is 0.3 m (12 in.).	22
3-11: Computed CO ₂ mass fraction contours colored by temperature below a 24 m x 24 m (80 ft x 80 ft) smooth ceiling inclined at 18.4° with a ridge located 6.1 m (20 ft) from the CUP array. CO ₂ mass fractions in the range of 0.02-0.04 are used. Ceiling is located 3.05 m (10 ft) above the CUP array.	23
3-12: Computed CO ₂ mass fraction contours colored by temperature below a 24 m x 24 m (80 ft x 80 ft) smooth ceiling inclined at 18.4° with a ridge located 12.2 m (40 ft) from the CUP array. Ceiling is located 3.05 m (10 ft) above the CUP array.	23
3-13: Computed CO ₂ mass fraction contours colored by temperature below a 24 m x 24 m (80 ft x 80 ft) obstructed ceiling inclined at 18.4° with a ridge located 6.1 m (20 ft) from the CUP array. Ceiling is located 3.05 m (10 ft) above the CUP array. Purlins of depth 0.2 m (8 in.) and 0.6 m (24 in.) deep girders present.....	24
3-14: Activation time contours of QR/OT sprinklers located 0.33 m (13 in.) below a smooth ceiling inclined at 9.5° with a ridge located (a) 6.1 m (20 ft), and (b) 12.2 m (40 ft) from the CUP array. Ceiling is 3.05 m (10 ft) above the CUP array.	25
3-15: Activation time contours of QR/OT sprinklers located 0.33 m (13 in.) below a smooth ceiling inclined at 18.4° with a ridge located (a) 6.1 m (20 ft), and (b) 12.2 m (40 ft) from the CUP array. Ceiling is 3.05 m (10 ft) above the CUP array.	26
3-16: Activation time contours of QR/OT sprinklers located 0.15 m (6 in.) below a smooth ceiling inclined at 18.4° with a ridge located (a) 6.1 m (20 ft), and (b) 12.2 m (40 ft) from the CUP array. Ceiling is 3.05 m (10 ft) above the CUP array.	27
3-17: Activation time contours of QR/OT sprinklers located 0.33 m (13 in.) below an obstructed ceiling inclined at 18.4° with a ridge located 6.1 m (20 ft) from the CUP array. Ceiling is 3.05 m (10 ft) above the CUP array.	28
3-18: Activation time contours of SR/HT sprinklers located 0.33 m (13 in.) below a smooth ceiling inclined at 18.4° with a ridge located (a) 6.1 m (20 ft), and (b) 12.2 m (40 ft) from the CUP array. Ceiling is 3.05 m (10 ft) above the CUP array.	29
4-1: Spray from an upright K160 sprinkler and the CUP array. The 0.61 m x 0.61 m (2 ft x 2 ft) sampling areas are also shown.	31
4-2: Instantaneous snapshots of sprays originating from the upright K160 sprinkler for (a) 0° inclination, deflector parallel to floor, (b) 18.4° inclination, deflector parallel-to-floor, and (c) 18.4° inclination, deflector parallel-to-ceiling. The 600-kW convective-HRR fire is shown by the instantaneous contour of the stoichiometric mixture fraction inside the rack-storage array.	33

4-3: Comparison of droplet mass flux distributions shown for a single upright K160 sprinkler when no fire is present and when a 600-kW convective-HRR fire is present. The sprinkler arms are oriented in the x-direction.	35
4-4: Time-averaged droplet mass flow rate through a 3.05 m x 3.05 m (10 ft x 10 ft) sampling area surrounding the ignition location at a height of 0.3 m (1 ft) above the CUP rack-storage array as a function of ceiling inclination. A single sprinkler is located above the ignition location: (a) without fire, and (b) with a fire of constant 600-kW convective HRR. Computed mass flow rates for an upright K160 sprinkler are compared against previous results for a pendent K200 sprinkler [1].	36
4-5: Instantaneous snapshots of sprays originating from four upright K160 sprinklers (two injection locations are visible in the images) for (a) 0° inclination, deflector parallel-to-floor, (b) 18.4° inclination, deflector parallel-to-floor, and (c) 18.4° inclination, deflector parallel-to-ceiling. The 2.6-MW convective-HRR fire is shown by the instantaneous contour of the stoichiometric mixture fraction.	38
4-6: Comparison of droplet mass flux distributions shown for four upright K160 sprinklers surrounding the ignition location when a 2.6-MW convective-HRR fire is present.	39
4-7: Time-averaged droplet mass flow rate through a 3.05 m x 3.05 m (10 ft x 10 ft) sampling area surrounding the ignition location at a height of 0.3 m (1 ft) above the CUP rack-storage array as a function of ceiling inclination. Four sprinklers are located below the ceiling with a fire of constant 2.6-MW convective HRR.	40
4-8: Instantaneous snapshots of sprays originating from the K240 sprinkler for (a) 0° inclination, deflector parallel to floor, (b) 18.4° inclination, deflector parallel-to-floor, and (c) 18.4° inclination, deflector parallel-to-ceiling. The 600-kW convective-HRR fire is shown by the instantaneous contour of the stoichiometric mixture fraction inside the rack-storage array.	41
4-9: Comparison of droplet mass flux distributions shown for a single pendent K240 sprinkler when no fire is present and when a 600-kW convective-HRR fire is present. The sprinkler arm is oriented in the x-direction.	42
4-10: Time-averaged droplet mass flow rate through a 3.05 m x 3.05 m (10 ft x 10 ft) sampling area surrounding the ignition location at a height of 0.3 m (1 ft) above the CUP rack-storage array as a function of ceiling inclination. A single sprinkler is located above the ignition location: (a) without fire, and (b) with a fire of constant 600-kW convective HRR. Computed mass flow rates for a pendent K240 sprinkler are compared against previous results for a pendent K200 sprinkler.	44
4-11: Instantaneous snapshots of sprays originating from four pendent K240 sprinklers (two injection locations are visible in the images) for (a) 0° inclination, deflector parallel-to-floor, (b) 18.4° inclination, deflector parallel-to-floor, and (c) 18.4° inclination, deflector parallel-to-ceiling. The 2.6-MW convective-HRR fire is shown by the instantaneous contour of the stoichiometric mixture fraction.	45
4-12: Comparison of droplet mass flux distributions shown for four pendent K240 sprinklers surrounding the ignition location when a 2.6-MW convective-HRR fire is present.	46
4-13: Time-averaged droplet mass flow rate through a 3.05 m x 3.05 m (10 ft x 10 ft) sampling area surrounding the ignition location at a height of 0.3 m (1 ft) above the CUP rack-storage array as a function of ceiling inclination. Four sprinklers are located below the ceilings with a fire of constant 2.6-MW convective HRR.	47

List of Tables

1-1: Parameters for the sprinkler activation simulations.	4
1-2: Additional parameters for the ridged-ceiling, sprinkler-activation simulations.....	4
1-3: Parameters for sprinkler-spray simulations.....	7
2-1: List of sprinkler activation parameters used in the present study.	11
3-1: Average activation times for four sprinklers surrounding the ignition location.....	21
3-2: Average activation times for the row of sprinklers on the near side of the ridge compared to sprinklers at the same location for the no-ridge case.	28

PAGE LEFT INTENTIONALLY BLANK

1. Introduction

In conjunction with the Property Insurance Research Group (PIRG) and in collaboration with the Fire Protection Research Foundation (FPRF), the research affiliate of the National Fire Protection Association (NFPA), this study investigates the impact of sloped ceilings with obstructed construction and ridges on fire protection requirements. The current study is aligned with the FPRF “Protection of Storage Under Sloped Ceilings – Phase 2” project. The goal of the FPRF project is to support the NFPA 13 Technical Committee and FM Global standards in the development of new protection requirements addressing sprinkler installation beneath sloped ceilings. Phase 2 of the project extends the parameter space covered in Phase 1 of the project [1], such as the inclusion of obstructed ceiling construction, ridges and analysis of the effect of ceiling slope on additional sprinklers types, etc. Based on the findings of the Phase 2 study, in combination with conclusions from the Phase 1 investigation, recommendations for large-scale test planning will be made.

In the Phase 1 study, smooth ceilings were considered and sprinkler activation and spray simulations were conducted. The following conclusions were made:

- Results from activation simulations using quick-response, ordinary temperature (QR/OT) sprinklers showed that ceilings up to and including 18.4° inclination have similar activation times and patterns as those of a horizontal ceiling for the four sprinklers immediately adjacent to the fire source. As for standard-response, high-temperature (SR/HT) sprinklers, the relatively greater activation delays may have an adverse impact on protection design.
- For spray calculations involving a single pendent sprinkler directly above the ignition location, it was found that the sprinkler deflector orientation, parallel to the ceiling or floor, strongly affects the water flux that reaches the fire source and the pre-wetting area. The parallel-to-floor deflector orientation was found to maintain a similar water-flux distribution to the fire region irrespective of the ceiling inclination.
- For a fire plume located among four sprinklers, it was determined that the ceiling slope of 33.7° adversely affects the overall spray density of both parallel-to-ceiling and parallel-to-floor orientations because of a highly-skewed activation pattern which results in the first four sprinklers activating on the elevated ceiling side.
- Considering the significant effect of the deflector orientation on the water flux for a pendent sprinkler above the ignition location and the relatively reduced effect of the orientation for the among-four sprinklers cases, the parallel-to-floor orientation is preferable for the cases studied in Phase 1 [1].

While Phase 1 focused on smooth, sloped ceilings, industrial facilities with obstructed ceiling construction are commonly found worldwide. Obstructed ceiling construction is defined as a ceiling assembly that prevents the hot gases produced during a fire event from reaching the nearest four ceiling-level sprinklers anywhere within a ceiling-level channel in a timely fashion [2]. See Figure 1-1(a) for an example of a channel formed by purlins. In this context, a channel is formed by structural ceiling members that extend down from the ceiling at least 0.1 m (4 in.) and are less than 70% open in cross-

sectional area. Additionally, the channel width needs to be less than the sprinkler spacing recommended by the applicable installation code for the ceiling to be considered obstructed (e.g., for a 3.05 m x 3.05 m or 10 ft x 10 ft recommended sprinkler spacing, the purlins need to be separated by <3.05 m or 10 ft). This type of construction is typically associated with the presence of purlins (see Figure 1-1(b) for details showing C- and Z-type purlins), girders, beams and other similar types of structural roof supporting materials at the ceiling level. Typical purlin depths range from 0.15 m (6 in.) to 0.36 m (14 in.). Warehouses are trending toward using deeper purlins. Other ceiling assemblies that result in obstructed ceiling construction use either steel beams or concrete tees.

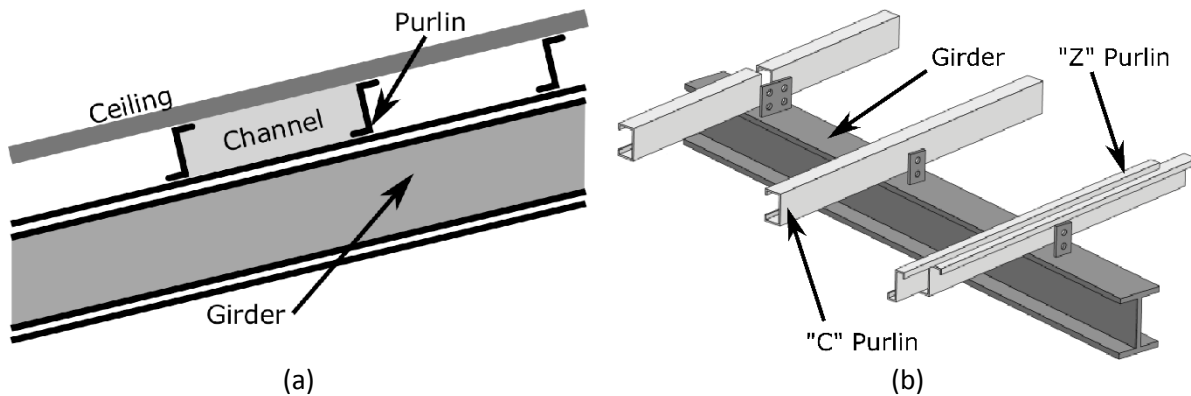


Figure 1-1: Obstructed ceiling construction present below a sloped ceiling: (a) purlins connected to the ceiling and a girder present along the ceiling slope, and (b) two types of purlin shapes (C- and Z-type) are shown connected to a girder.

A limited number of studies involving the presence of obstructed ceiling construction on fire protection design can be found in the literature. Bill et al. investigated the effect of sloped, beamed ceilings on residential sprinkler installation standards [3]. They conducted 32 fire tests in a compartment with home furnishings (e.g., reclining chair, curtains, etc.) as the fire source. Ceiling slope and presence of beams were determined to affect the sprinkler activations. However, it was found that, when the sprinkler sprays were not obstructed by the beams, fire spread was controlled in a similar fashion as when smooth, horizontal ceilings were used.

Davis et al. [4] conducted CFD simulations of beamed, sloped ceiling flows. Their investigation found that for beams perpendicular to the ceiling slope, the ceiling jet was impeded by the beams and there is channeling of the flow. As the beam depth increased, it was found that the channeling effect increased and the flow in the upward slope direction was affected. Vettori [5] experimentally investigated the effect of beams installed parallel to the ceiling slope and found that activation-time delays occurred in comparison to the smooth ceiling. In these experiments, the burner was placed such that the beams obstructed the ceiling jet in the direction of the sprinklers. In a recent study, Mealy et al. [6] conducted an experimental investigation using beamed, sloped ceilings and a fire heat release rate (HRR) of 100 kW. Smoke detector performance in the presence of beams of maximum depth 0.6 m (24 in.) was evaluated. It was found that such beam depths do not negatively affect expected detector performance when the detectors are located below the beams.

Besides the smaller-scale studies discussed above, the detailed effects of various obstruction depths and ceiling slopes on sprinkler activations for large-scale fires have not been investigated. Additionally, the presence of bounding surfaces such as ridges (peaks) may also affect sprinkler activation. Ridges can lead to accumulation of the fire products causing earlier activations to occur away from the fire location.

1.1 Objectives

The present study was undertaken to evaluate the effect of obstructed ceiling construction (e.g., purlins and girders) and ridges on sprinkler protection under sloped ceilings. The modeling-based investigation was conducted using the computational fluid dynamics (CFD) code FireFOAM [7] [8]. The numerical modeling work was performed by FM Global in collaboration with Fire and Risk Alliance [9], the FPRF contractor. The aim of the study was to provide guidance to the sprinkler installation standards and the large-scale tests planned in Phase 3 of the FPRF project by conducting the following:

- Evaluation of sprinkler activation times and patterns from ceiling jet simulations under ceilings having obstructed construction, ridges and a range of slopes, with large-scale growing fires as plume sources.
- Evaluation of the effect of ceiling inclination on water-flux distributions over a rack-storage commodity for upright- and pendent-type sprinklers.
- Understanding the effect of sprinklers oriented with the deflector parallel to the ceiling or to the floor.

1.2 Technical Approach

The modeling work was divided into two parts: 1) a sprinkler-activation study, and 2) a sprinkler-spray investigation, as described below.

For sprinkler activation predictions, simulations were performed of ceiling jets resulting from a growing fire on a 3-tier-high rack-storage array of FM Global Cartoned Unexpanded Plastic (CUP) commodity. Ceiling clearances of 3.05 m (10 ft) and 6.1 m (20 ft) were selected and ceiling inclinations between 0° and 18.4° were considered. Obstructed ceiling construction features in the form of purlins and girders were included in the simulations. Purlin depths of 0.1-0.6 m (4-24 in.) and a girder depth of 0.6 m (24 in.) were considered. Purlins and girders were separated by distances of 1.5 m (5 ft) and 7.6 m (25 ft), respectively. The ranges for ceiling clearance, inclination and obstruction depths were selected based on conclusions from the Phase 1 study [1] and considering prevailing storage conditions in the industry [10]. A summary of the parameters used in the sprinkler activation study is included in Table 1-1.

Table 1-1: Parameters for the sprinkler activation simulations.

Fire plume source		3-tier-high rack storage of CUP commodity (growing fire HRR)			
Ceiling clearances (h)		3.05 m (10 ft)			6.1 m (20 ft)
Ceiling	inclinations (θ)	0°	9.5°	18.4°	18.4°
	slopes	0	0.167 2 / 12 in.	0.333 4 / 12 in.	0.333 4 / 12 in.
Purlin	depths (d_p)	0.1-0.6 m (4-24 in.)			0.3 m (12 in.)
	separation distance (w_p)	1.5 m (5 ft)			
Girder	depth (d_g)	0.6 m (24 in.)			
	separation distance (w_g)	7.6 m (25 ft)			

Sprinkler activation simulations were also conducted with a ceiling containing a symmetrical ridge. The distance between the center of the commodity and the ridge was selected as 6.1 and 12.2 m (20 and 40 ft), measured along the slope of the ceiling. These distances were chosen to provide different levels of remoteness between the commodity and the ridge, and were based on two to four times the linear sprinkler spacing of 3.05 m (10 ft). Obstructed ceiling construction, in the form of 0.2 m (8 in.) deep purlins and 0.6 m (24 in.) deep girders, were included as well. Additionally, the effect of sprinkler stand-off distance on activations was considered. A summary of the additional parameters used in the obstructed ceiling sprinkler activation study is included in Table 1-2 below.

Table 1-2: Additional parameters for the ridged-ceiling, sprinkler-activation simulations.

Ceiling clearances (h)	3.05 m (10 ft)	
Ceiling inclinations (θ)	9.5°	18.4°
Ridge distance (w_r)	6.1, 12.2 m (20, 40 ft)	

Figure 1-2 below shows the computational setup with ceilings at different inclinations above a 3-tier-high rack-storage arrangement of CUP commodity. The purlins shown in the figure are in the perpendicular direction to the ceiling slope, whereas the girders are aligned with the slope. This arrangement was selected since in an overwhelming majority of warehouses such a structural design is followed. Open boundary conditions were simulated on all sides, leading to an unconfined ceiling. The ceiling configurations shown in the figure correspond to scenarios of the fire source being located far away from side walls or ridges, which tend to cause stagnation of the product gases and can lead to earlier activations. Construction elements in the form of purlins and girders below the ceilings provide obstruction to the ceiling jet.

Figure 1-3 below shows the computational setup of an obstructed, inclined ceiling with a ridge above the 3-tier-high rack-storage arrangement. The purlins and girders shown in the figure are in the same orientation shown in Figure 1-2. Smooth (i.e., without purlins and girders below the ceiling), inclined ceilings with a ridge were primarily simulated, and an additional simulation with the ridge in the presence of the obstructed ceiling construction was conducted.

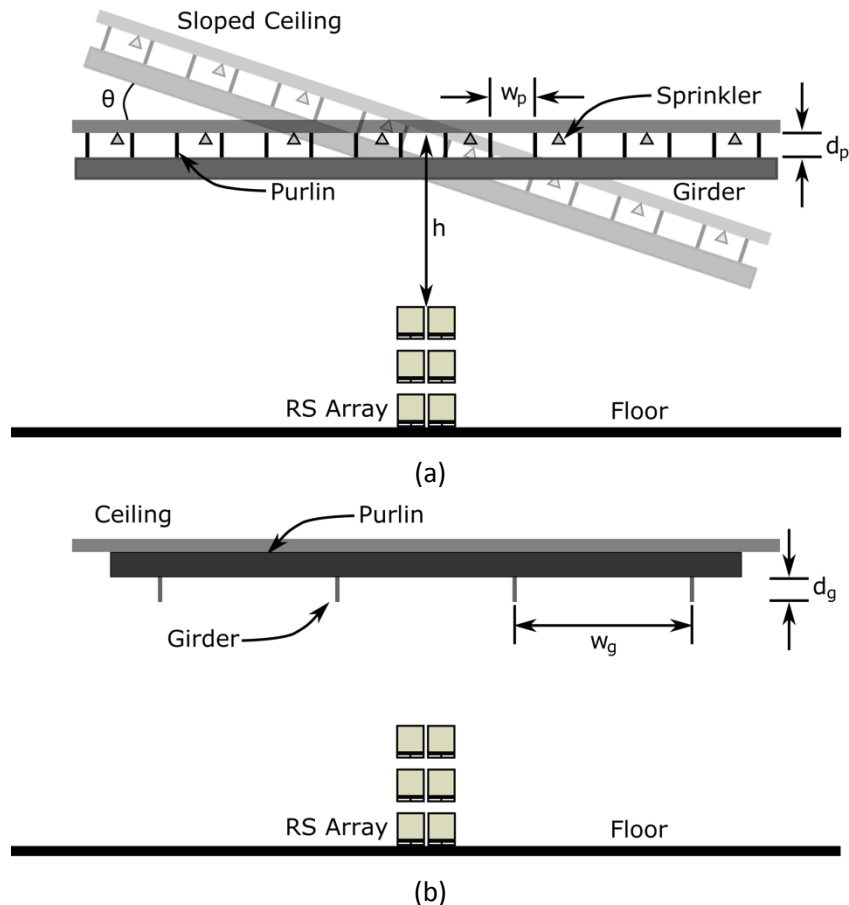


Figure 1-2: Computational setup (not to scale) showing the 3-tier-high rack-storage array: (a) front view showing purlins, girders and sprinklers below the ceilings (horizontal and inclined at θ angle), and (b) side view showing purlins and girders present below the horizontal ceiling.

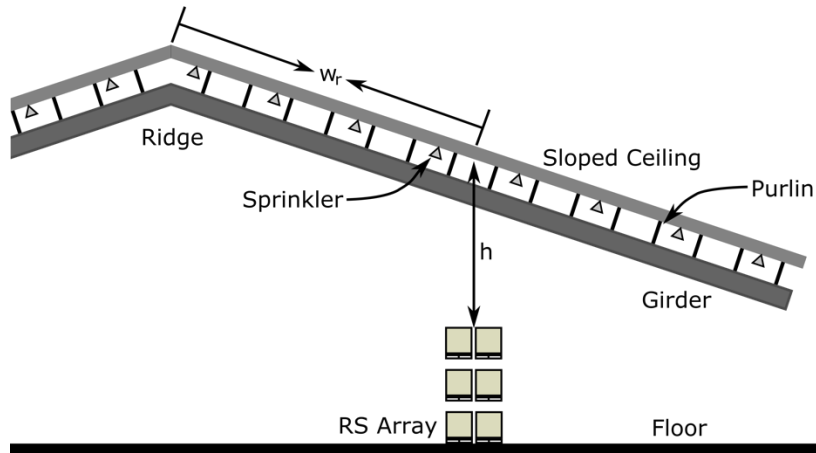


Figure 1-3: Computational setup (not to scale) showing a front view of the 3-tier-high rack-storage array with an inclined ceiling containing a ridge, purlins, girders and sprinklers below the ceiling.

The effect of slope and deflector orientation on sprinkler spray were also investigated for smooth ceilings. An upright K160 lpm/bar^{0.5} (K11.2 gpm/psi^{0.5}) and a pendent K240 lpm/bar^{0.5} (K16.8 gpm/psi^{0.5}) sprinkler were selected to complement the pendent K200 lpm/bar^{0.5} (K14.0 gpm/psi^{0.5}) sprinkler studied in Phase 1. The injection properties were obtained following a well-established characterization method [11]. The water-flux distribution reaching the top of the rack-storage array were simulated. The water-flux estimations were made for the ignition location under one sprinkler as well as among four sprinklers.

For the spray simulations, obstructed ceiling construction elements were not included since FM Globalⁱ [2] and NFPAⁱⁱ [12] recommendations ensure sprinkler installation locations are adjusted to eliminate spray obstructions caused by ceiling structural elements. Additionally, the initiation of sprinkler spray in these simulations does not rely on the ceiling jet for activation. Thus, the activation study and the spray study were effectively decoupled. A summary of the parameters used in the sprinkler-spray study is included in Table 1-3.

ⁱ FM Global Data Sheet 2-0: *Installation Guidelines for Automatic Sprinklers* (Sections 2.2.3.4.2 and 2.2.3.5).

ⁱⁱ NFPA 13: *Standard for the Installation of Sprinkler Systems* (Section 8.12.5).

Table 1-3: Parameters for sprinkler-spray simulations.

Fire plume source		3-tier-high rack storage of CUP commodity (fixed HRR)	
Ceiling clearance (H)		3.05 m (10 ft)	
Ceiling	inclinations (θ)	0°	18.4°
	slopes	0	0.333
Sprinkler type		Upright K160 lpm/bar ^{0.5} (K11.2 gpm/psi ^{0.5}) at 5.2 bar (75 psi) Pendent K240 lpm/bar ^{0.5} (K16.8 gpm/psi ^{0.5}) at 2.4 bar (35 psi)	
Deflector orientations		Parallel to ceiling	Parallel to floor

2. Numerical Model

2.1 FireFOAM Solver

FireFOAM [7], which is based on the open-source framework OpenFOAM [13], was used in the current study. OpenFOAM supports unstructured meshes with cells of arbitrary shapes permitting flexibility in ceiling jet mesh generation [14]. As in the Phase 1 study, the “saw-tooth” mesh used in other earlier studies [5] [15] [16] has been avoided in the current set of simulations.

FireFOAM includes models for large eddy simulation (LES) of buoyant turbulent diffusion combustion [8], pyrolysis [17] and radiation heat transfer [18]. Using FireFOAM, ceiling jets have been simulated for unconfined, smooth horizontal and inclined ceilings. Temperature and velocity predictions in the ceiling jets have also been validated using experimental data [1] [19] [20].

Multiphase-flow aspects of fire suppression are also included in FireFOAM. A Lagrangian transport model is employed to simulate water droplets originating from a sprinkler, transporting through fire plumes, and impinging on burnt and/or unburnt surfaces. A response time index (RTI) model has been included in FireFOAM and has been verified to give accurate estimates of sprinkler activation [21]. Actual delivered density (ADD) predictions have been made by the model [22] and suppression of rack-storage commodity has successfully been simulated [21] [23].

In the present study, the combustion, turbulent flow and radiation models are used to simulate the fire plumes and the resulting ceiling jets, and the Lagrangian model is used for sprinkler spray transport. The pyrolysis model was applied to generate the spatiotemporally varying fuel mass loss rates from a Cartoned Unexpanded Plastic (CUP) commodity (details available in Ref. [1]). Following the approach in the Phase 1 study, suppression simulations have not been conducted. FireFOAM version 2.2.x [7] has been used for the simulations.

2.2 Mesh Generation

The OpenFOAM version 3.0 mesh generation utility, *snappyHexMesh*, was used for mesh generation [14]. The *snappyHexMesh* utility generates three-dimensional meshes primarily composed of hexahedral volumes. The current set of meshes has been generated with the inclusion of Stereolithography (STL) geometries of boxes, pallets and horizontal/inclined ceilings, including the purlins and girders.

The purlin and girder structures have been simplified and details present in the actual structures (e.g., C- and Z-shaped purlins, I-beam structure for girders) are not included in the study, as such details will not significantly affect the flow dynamics. Instead, simplified vertical obstructions are considered: purlins are assumed to have 0.1 m (4 in.) width, and girders are assumed to be 0.2 m (8 in.) wide. Vertical depths of 0.1-0.6 m (4-24 in.) for the purlins are considered, whereas the girders are kept at a fixed depth of 0.6 m (24 in.). Details of the mesh generation steps are available in Ref. [1].

One primary difference exists between the meshes generated for the current study and the ones in Phase 1: the boundary layer mesh that was used earlier has not been included due to the presence of

the obstructed ceiling construction (see Figure 2-1). With increasing purlin depth, from 0.1 m (4 in.) to 0.6 m (24 in.), the total number of cells in the computational domain increased from ~2.6 million to ~4.1 million. Less than 4% of the generated cells were non-hexahedral (e.g., prisms and tet-wedges). The mesh resolution around the CUP rack-storage array was kept constant at 0.025 m (1 in.), whereas the uniform mesh below the ceiling (down to 0.3-0.6 m (12-24 in.) perpendicular distance) was kept at a 0.1 m (4 in.) resolution. The mesh resolution around the purlins and girders was between 0.025 m and 0.05 m (1 in.-2 in.). The plume region mesh was kept at a fixed resolution of 0.1 m (4 in.).

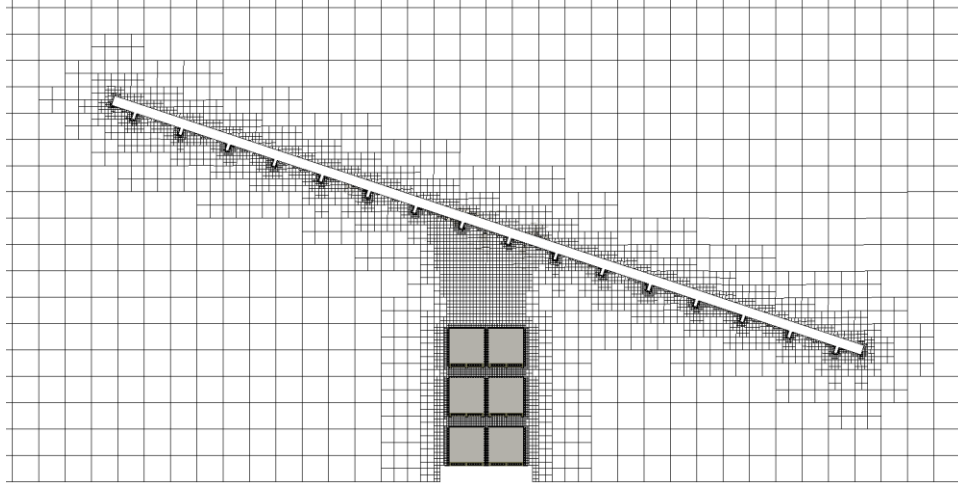


Figure 2-1: Computational mesh showing a ceiling inclined at 18.4° with its midpoint located 3.05 m (10 ft) above the rack-storage array. Purlins of a depth of 0.2 m (8 in.) are present below the ceiling.

2.3 Fire Growth Model

The transient fire growth modeling over the CUP rack-storage array was conducted with the application of a pyrolysis model for the CUP commodity [24] (see Ref. [1] for the model description). Following the approach in Phase 1, to expedite the simulation process in the current study, the pyrolysis model [24] was not directly applied. Instead, fire growth predictions were carried out using the full pyrolysis model and the resulting pyrolysis model output was saved. Then, for the sloped ceiling simulations a built-in “mapped-boundary” method in OpenFOAM was used to map the stored pyrolysis model output, thus avoiding a repeat calculation of the pyrolysis model. The mapping process is described in detail in Section 2.3.1 of Ref. [1].

Using the mapped boundary condition for pyrolysis, fire growth simulations under various ceiling configurations have been conducted. In Figure 2-2 the fire at 100 s, represented by the stoichiometric mixture fraction value, is shown impinging on an inclined ceiling with purlins and girders. The fire chemical HRR reaches ~17 MW at 100 s and the peak HRR is ~25 MW at 150 s, as shown in Figure 2-3. Correspondingly, the convective HRR at 100 s is ~12 MW and its peaks value is ~15 MW at 150 s. The radiant fraction, also shown in Figure 2-3, varies with time, beginning with a 0.5 value for the igniter, then reducing to ~0.22 for corrugated burning and finally approaching ~0.35 with increased burning of the polystyrene cups inside the cartons.

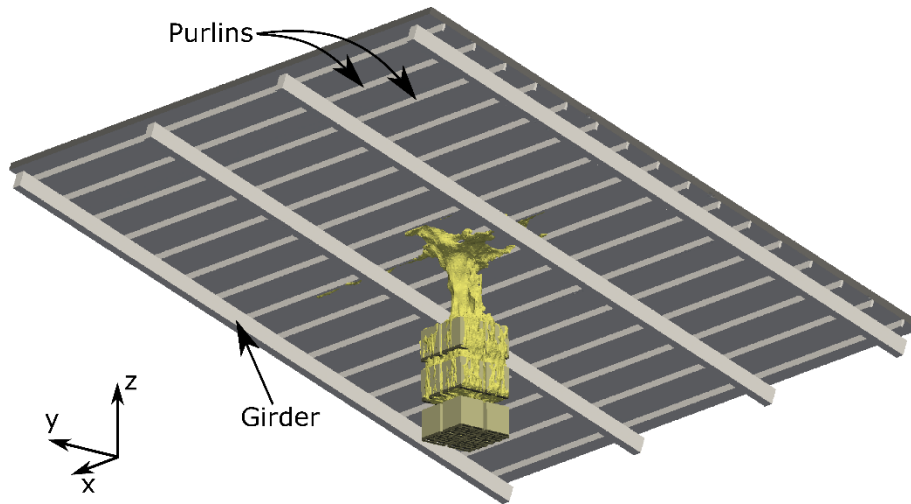


Figure 2-2: Fire impinging on a ceiling with 0.2 m (8 in.) purlins and 0.6 m (24 in.) girders present. The ceiling is inclined at 18.4°.

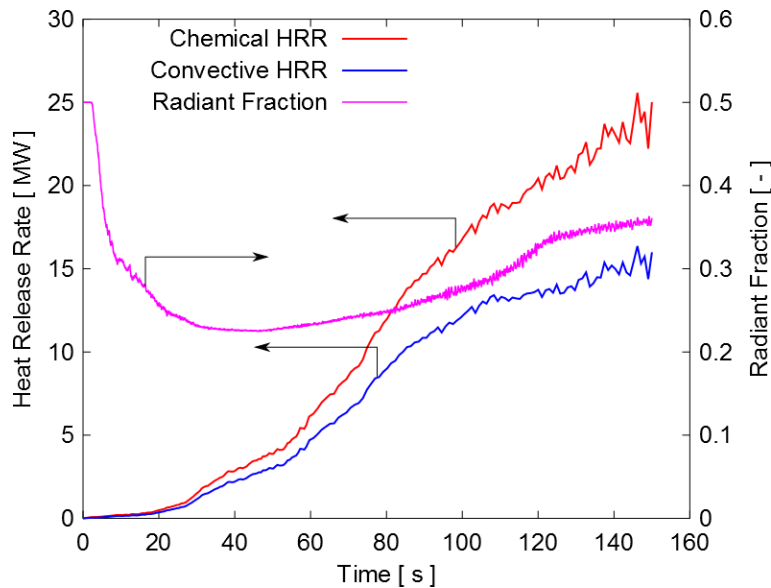


Figure 2-3: Modeled HRR (chemical and convective) and radiant fraction variation in time for the 2 x 2 x 3 array of CUP commodity.

As described above, the pyrolysis region uses mapped boundary conditions for velocity, temperature and pyrolysis species. The ceiling, including the purlins and girders, were treated as inert walls, with an isothermal temperature boundary (at 298.15 K) and a no-slip condition for velocity. The open boundaries on the sides were kept far away from the ceiling and rack-storage locations. The downstream outlet boundary was also kept sufficiently far away from the top of the inclined ceiling locations so as not to affect the flow.

2.4 Sprinkler Activation Setup

Sprinkler activations were simulated with calculations based on the RTI value. A scalar field variable for activation time, t_{act} , was used to record potential activation times at each location in the computational mesh. Activation patterns based on the t_{act} field values were extracted for a plane parallel to the inclined ceiling, located at a perpendicular distance of 0.33 m (13 in.) to the flat part of the ceiling. In addition, when the ridge is present below the ceiling, activation patterns are also presented at a distance of 0.15 m (6 in.). These results provide detailed, spatial contours of activation times, as described in Section 3. Activation times for a sprinkler layout corresponding to ignition among four sprinklers are also presented. These times were extracted by probing the t_{act} field at specified locations. Activation times for other sprinkler layouts (e.g., 2.4 m x 3.7 m or 8 ft x 12 ft) can be extracted in a similar way.

Two types of sprinklers were evaluated: the primary analysis was conducted with a quick-response sprinkler having an ordinary activation temperature (henceforth referred to as a QR/OT sprinkler), and for comparison purposes a standard-response sprinkler with a high activation temperature (henceforth referred to as an SR/HT sprinkler) was also selected. The sprinkler characteristics were selected to cover the wide range of RTI and activation temperature combinations available for these sprinklers. Details of the sprinklers are given in Table 2-1. Following the concept of isolating the activation patterns from suppression phenomena, as described in Section 2.5 of Ref. [1], for the activation calculations, sprinkler sprays were not included.

Table 2-1: List of sprinkler activation parameters used in the present study.

Name	Response	Activation Temperature K (°F)	RTI (m-s) ^{0.5} ((ft-s) ^{0.5})	C-Factor (m/s) ^{0.5} ((ft/s) ^{0.5})
QR/OT	Quick	347 (165)	30 (54)	0.22 (0.40)
SR/HT	Standard	414 (286)	119 (216)	0.95 (1.72)

2.5 Sprinkler Spray Setup

For the sprinkler spray simulations, an injection profile developed following the measurements of Zhou et al. [11] was applied for two sprinklers: upright K160 lpm/bar^{0.5} (K11.2 gpm/psi^{0.5}) and pendent K240 lpm/bar^{0.5} (K16.8 gpm/psi^{0.5}). The upright sprinkler, henceforth referred to as “K160”, was selected to compare the water-flux distribution obtained using the pendent K200 lpm/bar^{0.5} (K14 gpm/psi^{0.5}) sprinkler (henceforth referred to as “K200”) used in the Phase 1 study. An additional pendent sprinkler with a higher K-factor (K240 lpm/bar^{0.5} or K16.8 gpm/psi^{0.5}) was also included (known henceforth as “K240”) as it is more prevalent in the industry. The injection profile was applied in the hemispherical region located 0.1 m (0.33 ft) below the sprinkler deflectors. Two scenarios have been simulated:

- One sprinkler above the ignition location: water-flux distributions recorded 0.3 m (1 ft) above the CUP array with and without the presence of a 600-kW convective-HRR fire source.
- Four sprinklers surrounding the ignition location (3.05 m x 3.05 m or 10 ft x 10 ft spacing): water-flux distributions recorded in the presence of a 2.6-MW convective-HRR fire source.

In both scenarios, two sprinkler deflector orientations are considered: deflector parallel to the floor or to the ceiling.

3. Sprinkler Activation Study

In this work, sprinkler activations are simulated by disabling the suppression physics (spray injection, spray transport, thin film flow, etc.) in FireFOAM. This follows the approach taken in Phase 1 of the study [1]. This approach allows isolation of the fire-plume effect on the sprinkler-activation patterns.

Activations from the CUP rack-storage fire plume are simulated in accordance with the parameters in Table 1-1 for obstructed construction (purlins and girders). The results are compared against activations for smooth ceilings at the same inclinations. Activations in the presence of ceiling ridges are next described using the parameters in Table 1-2. Obstructed construction (purlins and girders) are also included along with the ridge. Flow characteristics in the presence of obstructed ceiling construction and ridges are described and trends in the ceiling jet development are discussed. Activation patterns and times for two types of sprinklers, QR/OT and SR/HT, are next presented with recorded trends discussed. The observations are summarized at the end of the section.

3.1 Ceiling Flows in Presence of Obstructed Construction

3.1.1 Ceiling Jet Development

A thermal boundary layer below the ceiling is generated by the transient plume originating from the CUP rack-storage fire. For describing the flow below obstructed ceilings, an inclination of 18.4° is considered and development of the ceiling jet when obstructed ceiling construction is present is compared with the case of a smooth ceiling. In Figure 3-1, instantaneous contours of CO_2 mass fractions ($Y_{\text{CO}_2} = 0.02-0.04$), used as a tracer for illustrating the ceiling jet, are shown below a smooth ceiling with its mid-point 3.05 m (10 ft) above the top of the CUP array. The contours are colored by temperature in the range of $400 \text{ K} \leq T \leq 1200 \text{ K}$. As observed in Figure 3-1(a), at an early time of 40 s, the higher temperature region is confined to the ceiling center. With increasing time, as observed in Figure 3-1(b-d), a skewness in ceiling jet development can be observed on the elevated section. The widening of the ceiling jet is also observed in Figure 3-1(c-d), particularly on the elevated side.

When obstructed ceiling construction in the form of the 0.6 m (2 ft) deep girders and 0.1 m (4 in.) purlins are present, as shown in Figure 3-2, the ceiling jet tends to develop along the channels formed by the girders and to a lesser extent along the channels formed by the purlins. As observed in Figure 3-2(c-d), the ceiling jet predominantly remains confined in the channel formed by the two central girders. The slope affects the ceiling jet and a flow skewed toward the elevated side also expectedly occurs. The small opening between the girders and the ceiling (as caused by the presence of the purlins) allows some flow to move laterally outwards, but most of the flow outside of the central girder channel occurs due to spillage under the girders, as can be observed in Figure 3-2(c-d). The girders provide a channeling effect and the flow remains confined between them. The presence of the 0.1 m (4 in.) deep purlins does not affect the flow significantly, as the main effect is that of the girders. These trends hold true when the purlin depth is doubled to 0.2 m (8 in.) (see Figure 3-3).

Increasing the purlin depth to 0.3 m (12 in.) causes the ceiling jet to stay confined in the purlin channels. Only at times greater than 80 s is some flow along the elevated side observed, as can be seen in Figure 3-4(c-d). For the most part though, the ceiling jet develops in the central purlin channels. Doubling the purlin depth again to 0.6 m (24 in.) shows that the effect of the girder channel or the ceiling slope is not strong on the ceiling jet, as now the purlin depth is too deep for the effect of the girders or the slope to be felt (see Figure 3-5). The core flow region remains confined in the central purlin channels.

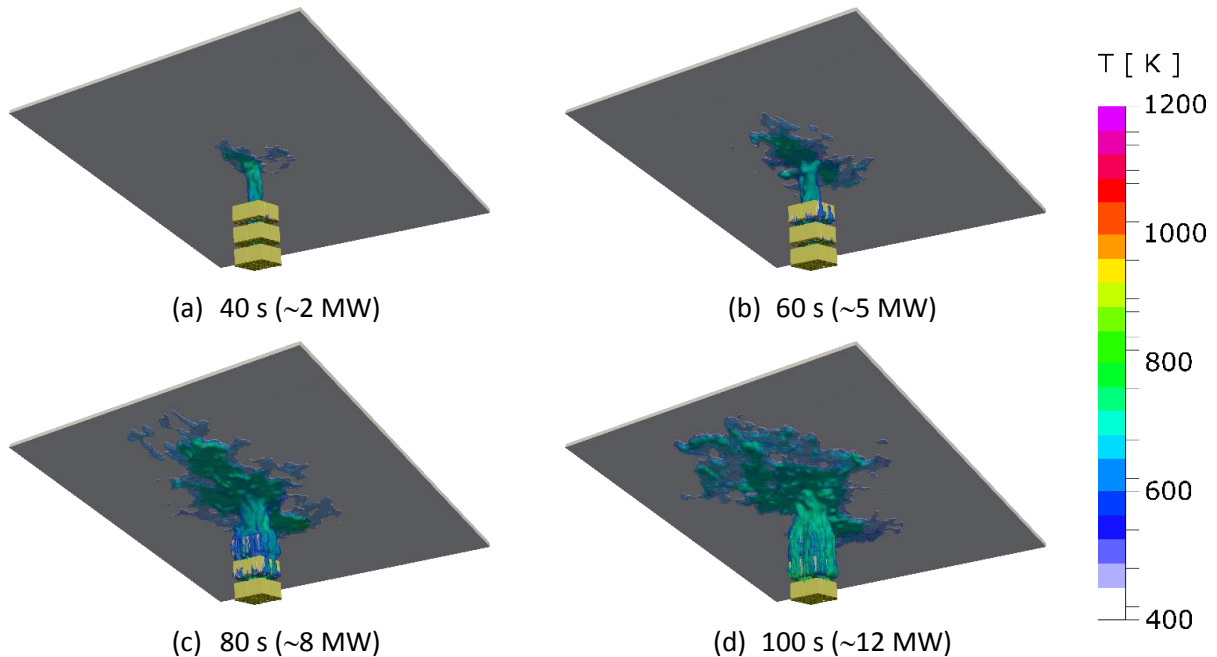


Figure 3-1: Computed CO₂ mass fraction contours colored by temperature below a 24 m x 24 m (80 ft x 80 ft) smooth ceiling inclined at 18.4° located 3.05 m (10 ft) above the CUP array. Approximate convective HRR at the selected times are also shown.

3.1.1 Activations of Quick-Response, Ordinary Temperature Sprinklers

Activation times and patterns are presented in Figure 3-6 for QR/OT sprinklers for ceilings in the presence of obstructed ceiling construction. Activation times are shown for a selected arrangement that surrounds the ignition location with four sprinklers (henceforth known as the “among-four” sprinkler configuration). The activation time contours shown in the figure are for the case of a horizontal ceiling located 3.05 m (10 ft) above the top of the 2 x 2 x 3 CUP rack-storage array. The contours are for a plane parallel to and located 0.33 m (13 in.) below the ceiling, representing the maximum sprinkler thermal-element offset for sprinklers with K-factor 240 (16.8) and lower.

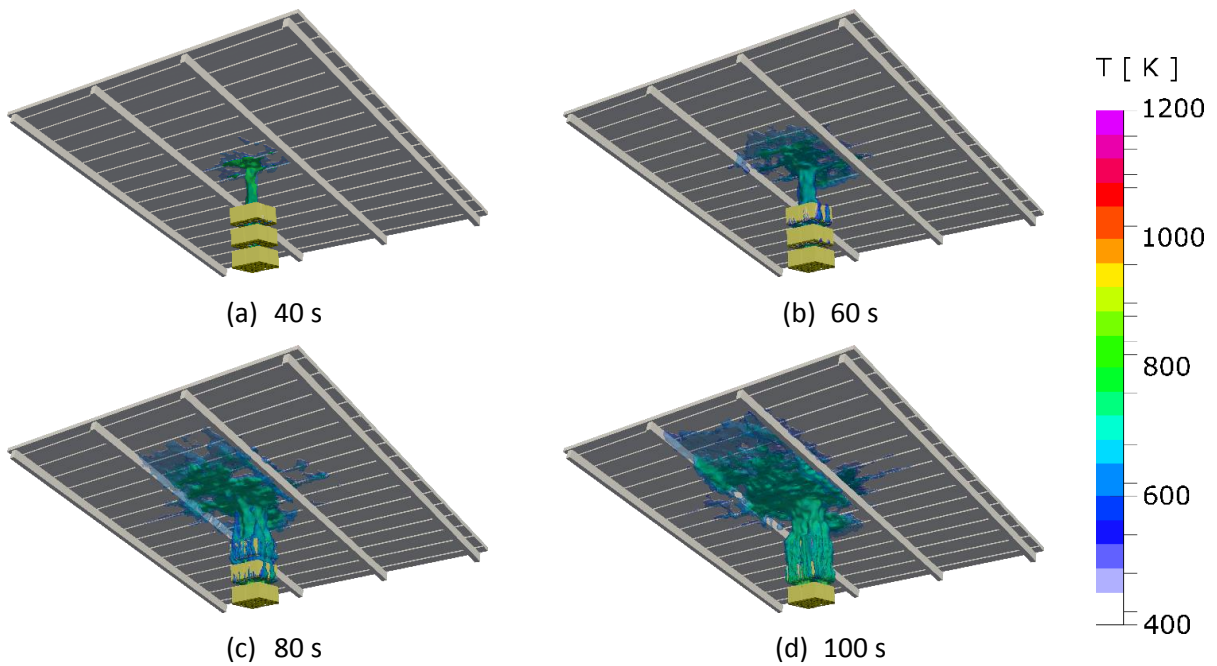


Figure 3-2: Computed CO₂ mass fraction contours colored by temperature below a 24 m x 24 m (80 ft x 80 ft) ceiling inclined at 18.4° with 0.1 m (4 in.) deep purlins located 3.05 m (10 ft) above the CUP array.

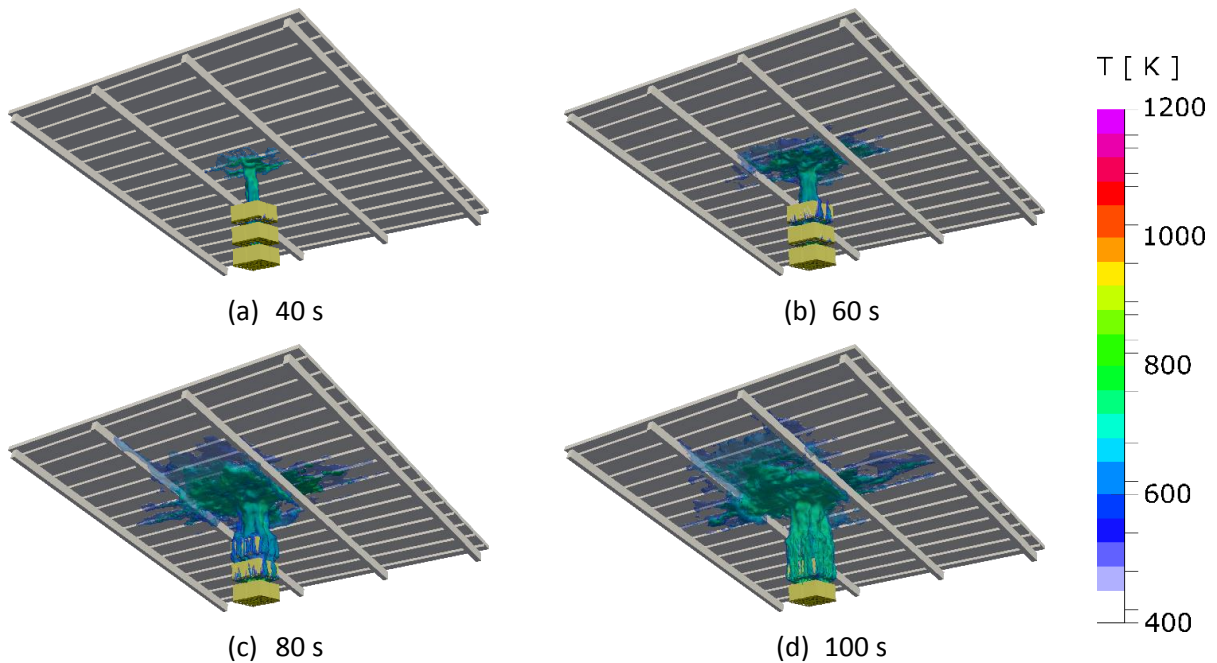


Figure 3-3: Computed CO₂ mass fraction contours colored by temperature below a 24 m x 24 m (80 ft x 80 ft) ceiling inclined at 18.4° with 0.2 m (8 in.) deep purlins located 3.05 m (10 ft) above the CUP array.

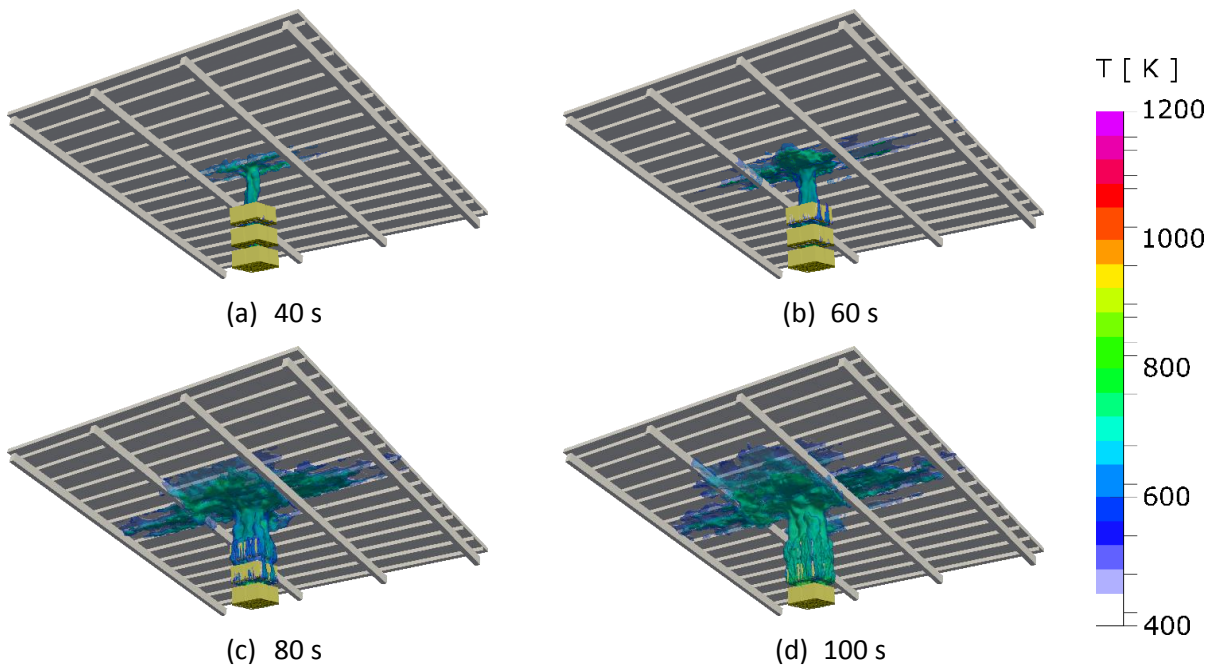


Figure 3-4: Computed CO₂ mass fraction contours colored by temperature below a 24 m x 24 m (80 ft x 80 ft) ceiling inclined at 18.4° with 0.3 m (12 in.) deep purlins located 3.05 m (10 ft) above the CUP array.

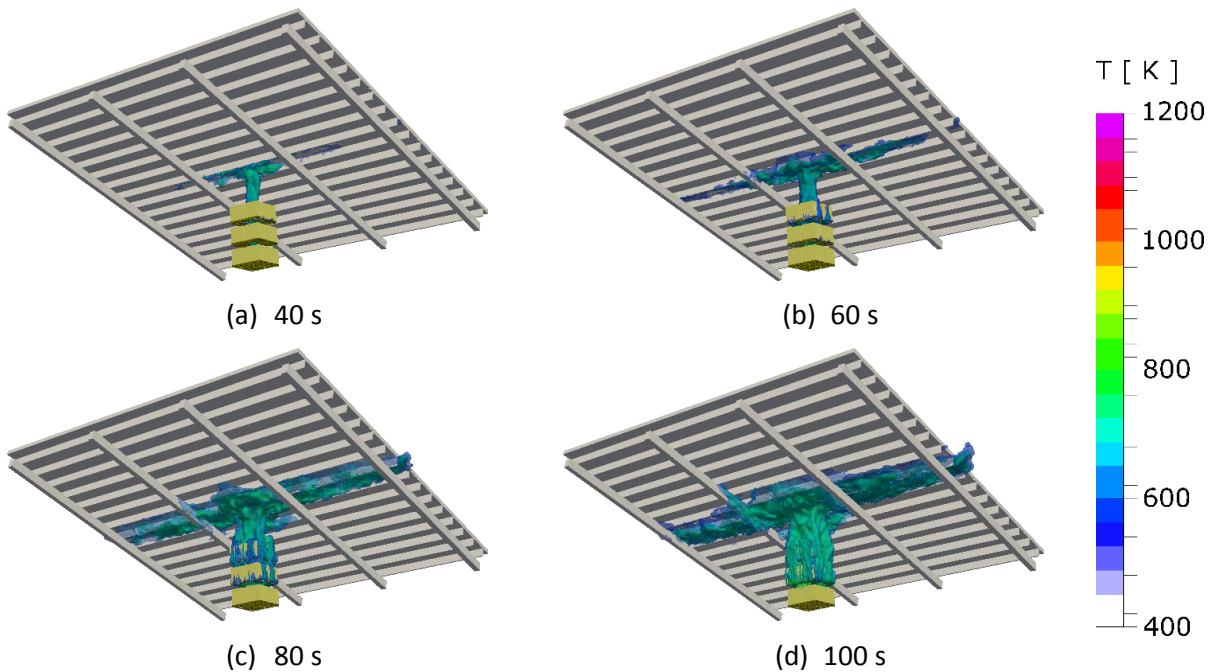


Figure 3-5: Computed CO₂ mass fraction contours colored by temperature below a 24 m x 24 m (80 ft x 80 ft) ceiling inclined at 18.4° with 0.6 m (24 in.) deep purlins located 3.05 m (10 ft) above the CUP array.

3.1.1.1 Horizontal Ceiling

In Figure 3-6(a), activation contours are shown for a case with a purlin depth of 0.1 m (4 in.) present below a horizontal ceiling. The purlins and girders are shown overlaid on the contours. Activation times are primarily affected by the presence of the girders that enable channeling of flow in the direction perpendicular to the purlins. Activation times beyond the plume impingement region, approximately up to 12 m (40 ft) from the mid-point of the ceiling in the direction perpendicular to the purlins, increase by approximately 10-12 s.

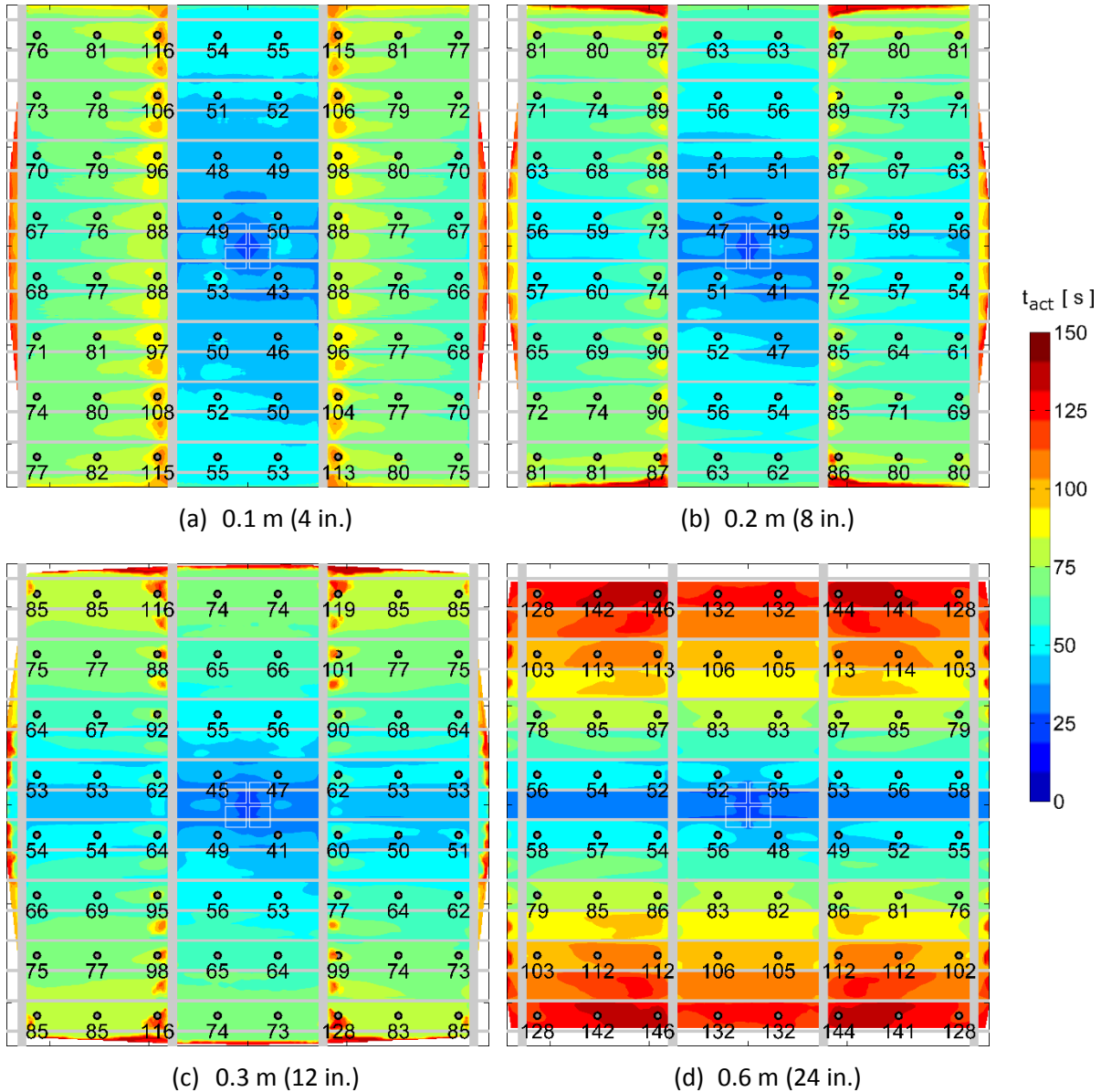


Figure 3-6: Activation of QR/OT sprinklers located 0.33 m (13 in.) below a horizontal ceiling 3.05 m (10 ft) above the CUP array when purlin depth is (a) 0.1 m (4 in.), (b) 0.2 m (8 in.), (c) 0.3 m (12 in.), and (d) 0.6 m (24 in.). Purlins and girders are overlaid on top of the contours. Ceiling is 24 m x 24 m (80 ft x 80 ft).

The activation times in the first ring (the four sprinklers surrounding the ignition location) are not significantly affected by doubling the purlin depth from 0.1 m (4 in.) to 0.2 m (8 in.). The open area between the girder and the ceiling doubles for the 0.2 m (8 in.) purlins. Flow escapes through this area causing earlier activations to occur in the purlin channels, outside the central girder region.

Increasing the purlin depth to 0.3 m (12 in.), as can be seen in Figure 3-6(c), activation time delays between 7-32 s are observed in the direction perpendicular to the purlins. However, the average activation time for the first ring is not significantly affected. The ceiling jet tends to travel in the channels formed by the purlins. A distinct difference between activation patterns for purlin depths <0.3 m (12 in.) and ≥ 0.3 m (12 in.) can be observed as well. For purlin depths <0.3 m (12 in.), the channeling effect is primarily due to the presence of the girders, whereas for depths ≥ 0.3 m (12 in.) the flow predominantly moves in the channels formed by the purlins.

For the deepest purlins considered in the study, of a depth of 0.6 m (24 in.), the channeling of the ceiling jet along the purlins is the dominant phenomenon as indicated by the activation pattern in Figure 3-6(d). The sprinklers along the purlin channels activate within few seconds of each other. For sprinkler links beyond the first ring present 0.33 m (13 in.) below the ceiling, activation delays in the direction perpendicular to the purlins increase by 31-67 s. If the sprays from the activated sprinklers in the first ring cannot slow down the fire growth rate, these activation delays may result in an out of control fire spread.

3.1.1.2 Inclined Ceiling (9.5°)

With the ceiling inclined at 9.5°, activation patterns in the presence of obstructed ceiling construction are skewed toward the elevated side as was the case for the smooth ceiling results reported in Ref. [1]. In Figure 3-7, activation times and patterns are shown. For a purlin depth of 0.1 m (4 in.) as observed in Figure 3-7(a), the average activation time for the sprinklers in the first ring reduces by ~2.5 s compared to a smooth ceiling inclined at 9.5°. For sprinklers beyond the first ring and located on the elevated ceiling side, activations compared to the horizontal ceiling with the same purlin depth (Figure 3-6(a)) occur at earlier times. This is due to the ceiling jet turning upwards. A contrary behavior is observed for the sprinklers on the non-elevated side where activation times compared to the horizontal ceiling case are delayed significantly: activation delays of 24-44 s are observed for sprinklers beyond the first ring. Due to the flow turning upwards, the outermost sprinklers on the lower ceiling side do not activate.

For the 0.3 m (12 in.) purlins as shown in Figure 3-7(c), the channeling effect that was observed for the horizontal ceiling with the same purlin depth is again observed. However, the inclined ceiling causes the channeling effect to be significant only on the elevated ceiling side. Activations on the elevated ceiling side occur with greater delays compared to the cases with purlin depths <0.3 m (12 in.). Skewness between the elevated and non-elevated ceiling side activations also increases. The average activation time for the two elevated sprinklers adjacent to the ignition location initially decreases when the purlin depth increases from 0.1 m (4 in.) to 0.2 m (8 in.) and then increases for the 0.3 m (12 in.) purlin case. As the ceiling jet impinges on the purlins, it thickens and flow spills into the adjacent channels causing

earlier activations to occur. However, with increasing purlin depth, the channeling effect is greater and the spillover to the adjacent channels is delayed.

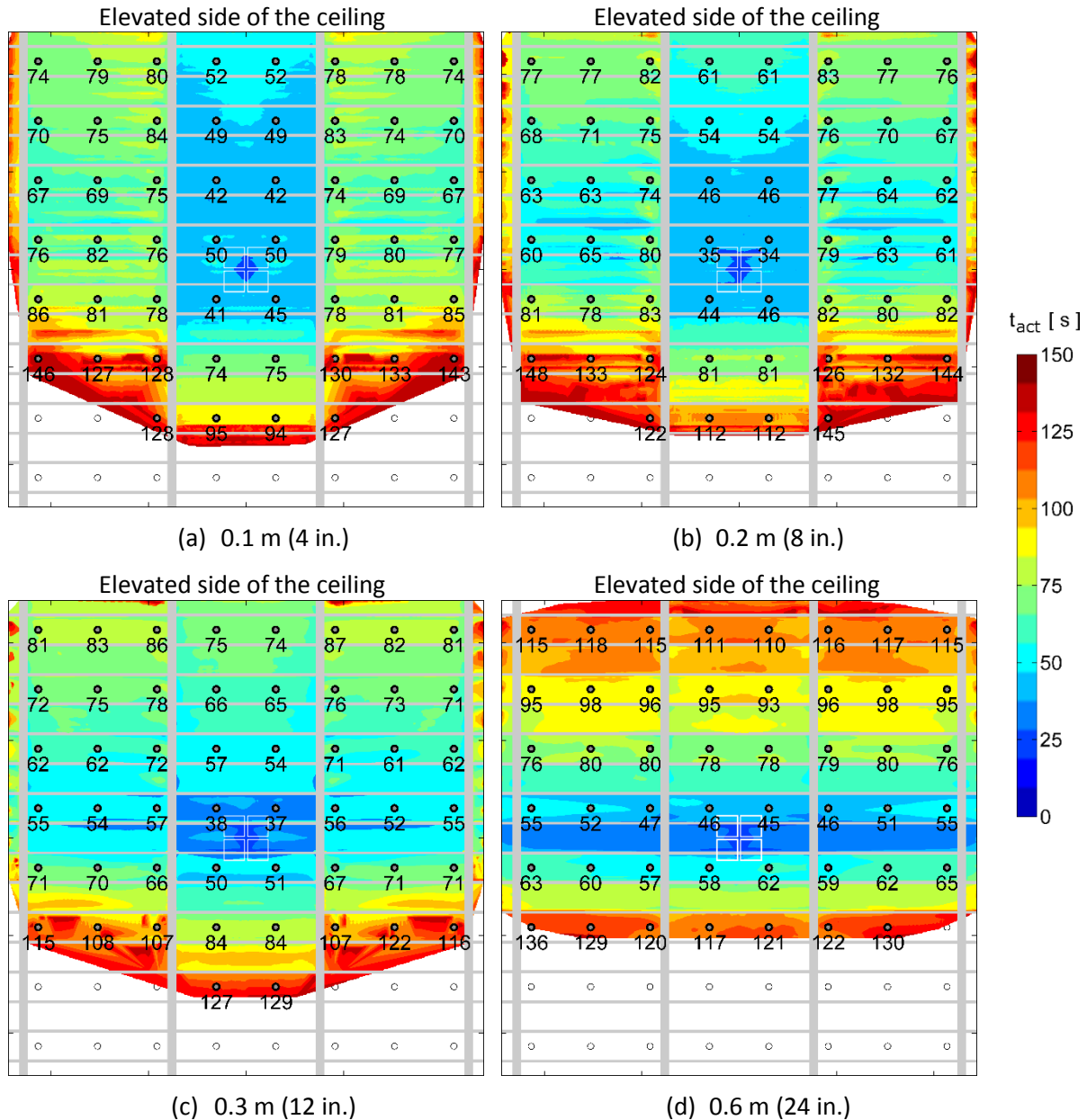


Figure 3-7: Activation of QR/OT sprinklers located 0.33 m (13 in.) below a ceiling inclined at 9.5° with its midpoint 3.05 m (10 ft) above the CUP array when purlin depth is (a) 0.1 m (4 in.), (b) 0.2 m (8 in.), (c) 0.3 m (12 in.), and (d) 0.6 m (24 in.). Purlins and girders are overlaid on top of the contours.

For the 0.6 m (24 in.) purlins shown in Figure 3-7(d), activation times along a single purlin channel are almost similar with no activations for the outermost two rows of sprinklers on the lower ceiling side. Activations in each purlin channel on the elevated ceiling side occur at earlier times compared to the

horizontal ceiling case with the same purlin depth. The activation delays in the direction perpendicular to the purlins, on the elevated ceiling side, increase compared to when the purlin depths are <0.6 m (24 in.).

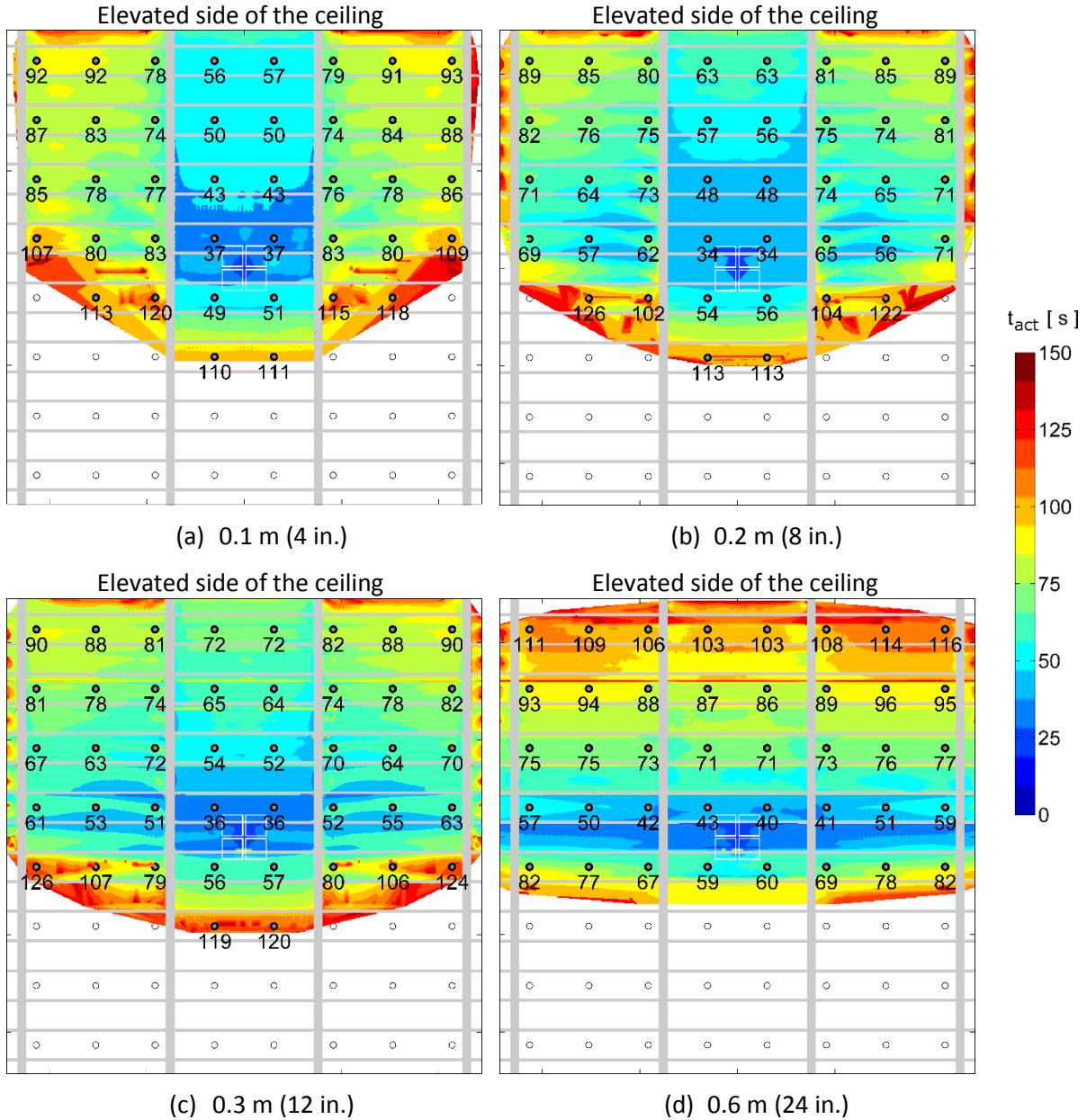


Figure 3-8: Activation of QR/OT sprinklers located 0.33 m (13 in.) below a ceiling inclined at 18.4° with its midpoint 3.05 m (10 ft) above the CUP array when purlin depth is (a) 0.1 m (4 in.), (b) 0.2 m (8 in.), (c) 0.3 m (12 in.), and (d) 0.6 m (24 in.). Purlins and girders are overlaid on top of the contours.

3.1.1.3 Inclined Ceiling (18.4°)

When the ceiling inclination is increased to 18.4°, the skewness in the sprinkler activation pattern increases with a lesser number of sprinklers activating on the non-elevated ceiling side as can be seen in Figure 3-8. The activation-region shrinks compared to when a smooth ceiling is inclined at 18.4° (see Figure 3-9 in Ref. [1] showing the activation contours for the smooth ceiling). For the same purlin depth, activations above the ignition region on the elevated side occur earlier compared to the 9.5° inclination cases, whereas outside the central girders the activation times are not significantly affected by the slope increase.

For the 0.1 m (4 in.) purlin case, as shown in Figure 3-8(a), almost six activations on the elevated ceiling side occur before the first two activations occur on the non-elevated side. The skewness compared to the smooth ceiling inclined at 18.4° [1] increases considerably, and can be attributed to the presence of girders.

Increasing the purlin depth to 0.3 m (12 in.) results in the obstruction of the ceiling jet by the purlins located on the elevated ceiling side, causing significant activation delays, as can be seen in Figure 3-8(c). The skewness between the elevated and non-elevated sprinklers closest to the ignition location also increases with an average difference of 20 s observed. For the largest purlin depth of 0.6 m (24 in.), the activation times on the elevated side increase significantly compared to when a smooth ceiling inclined at 18.4° is considered. The skewness between the elevated and non-elevated side sprinklers also increases considerably.

From this part of the study, the following conclusions can be made for QR/OT sprinklers:

- At small purlin depths of 0.2 m (8 in.) and less, the ceiling-jet flow is channeled by the girders toward the elevated direction.
- With increasing purlin depth and for a given ceiling inclination, the ceiling jet tends to increasingly develop along the purlin channels.
- For increasing inclination and purlin depth ≤ 0.3 m (12 in.), activation times on the elevated ceiling side in the central region between the girders do not change significantly.
- For the 18.4° inclination case, activation times are considerably skewed towards the elevated ceiling side. For purlin depths ≥ 0.3 m (12 in.), more activations occur along the purlin channels on the elevated side immediately above the ignition location.

3.1.1.4 Comparison with Smooth Ceiling Activation Times

To compare the combined effect of purlin depth and ceiling inclination on the activation performance of QR/OT sprinklers, the activation times for the four sprinklers surrounding the ignition location are considered. In Table 3-1, the average activation times are reported for the horizontal and inclined ceilings. For the inclined ceilings, the average activation times for the two elevated and non-elevated sprinklers are also presented using the \pm symbol: e.g., in case of the 9.5° ceiling with no purlins, the activation time reported is 49 ± 2 , where the average activation time for the four sprinklers is 49 s, the elevated sprinklers activation time is 2 s earlier and the non-elevated sprinklers activate 2 s later.

For the horizontal ceiling, the average activation time initially decreases with increasing purlin depth and then increases for depths >0.3 m (12 in.). This same trend is noticeable for the two inclined ceilings as well. However, for the inclined ceilings, when the purlin depth increases, the skewness between the elevated and non-elevated sprinklers increases substantially. For the 18.4° ceiling with purlin depths ≥0.2 m (8 in.), activations on the non-elevated side occur ~20 s after the elevated sprinklers have operated. This activation skewness may result in poor suppression performance on the non-elevated ceiling side.

Table 3-1: Average activation times for four sprinklers surrounding the ignition location.

Inclination (°)	Purlin depth (m)				
	0	0.1	0.2	0.3	0.6
0	49	49	47	46	53
9.5	49±2	47±4	40±5	44±7	53±7
18.4	46±2	44±7	45±11	46±10	51±9

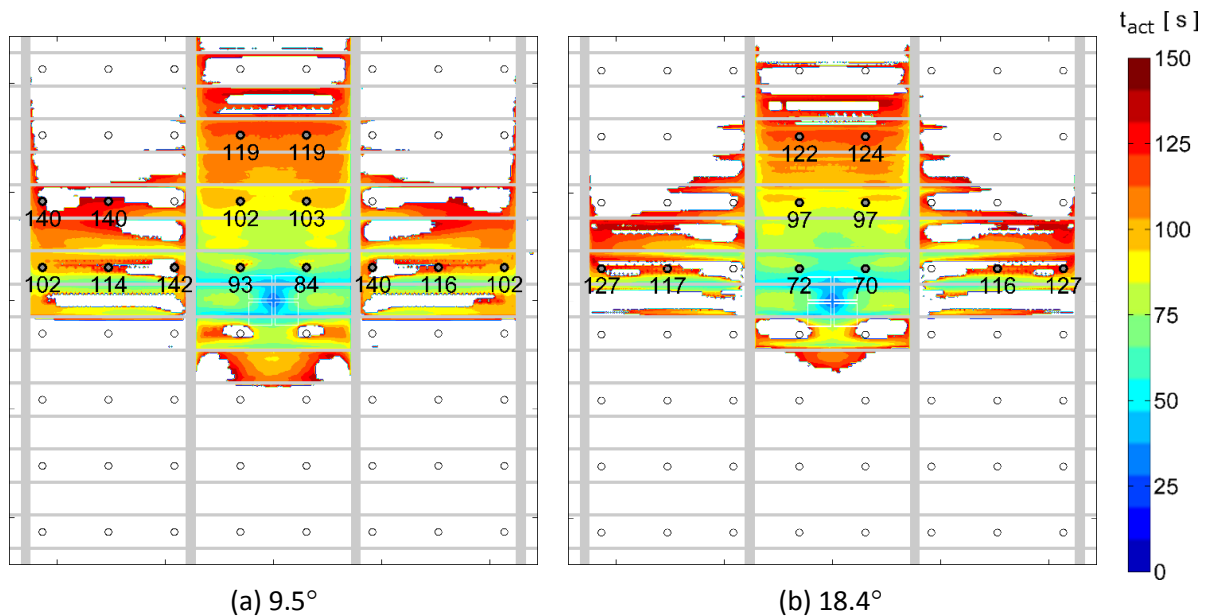


Figure 3-9: Activation of SR/HT sprinklers located 0.33 m (13 in.) below ceilings with their midpoints 3.05 m (10 ft) above the CUP array when purlin depth is 0.3 m (12 in.). Ceiling inclinations are (a) 9.5°, and (b) 18.4°. Purlins and girders are overlaid on top of the contours.

3.1.2 Activations of Standard-Response, High Temperature Sprinklers

For standard-response, high temperature (SR/HT) sprinklers, the activation time patterns are presented for two ceiling inclinations—9.5° and 18.4°—and a purlin depth of 0.3 m (12 in.). In Figure 3-9(a), activation patterns are shown for the 9.5° case. Compared to the QR/OT sprinklers, the region where SR/HT sprinklers will activate shrinks. For the two sprinklers immediately adjacent to the ignition

location on the elevated side, an average activation delay of ~51 s is observed when compared to the QR/OT sprinklers (see Figure 3-7(c) for values). None of the sprinklers on the non-elevated ceiling side activate. Most of the sprinklers on the elevated side also do not activate.

Increasing the ceiling inclination to 18.4° causes the region of activations on the elevated ceiling side to become smaller, as observed in Figure 3-9(b). The two elevated sprinklers closest to the ignition location activate at earlier times, influenced by the greater flow velocities encountered on the elevated ceiling side due to the higher ceiling inclination. It can be concluded, based on the skewed activation patterns observed, that SR/HT sprinklers would provide lower suppression performance compared to the QR/OT sprinklers for a given purlin depth.

3.1.3 Effect of Ceiling Clearance

For an inclination angle of 18.4° and purlin depth of 0.3 m (12 in.), increasing the clearance from 3.05 m (10 ft) to 6.1 m (20 ft) results in the average time difference between the elevated and non-elevated QR/OT sprinklers adjacent to the ignition location to increase marginally from 20.5 s to 23 s. The average activation time for the four sprinklers surrounding the ignition location increases to 51.5 s as compared to the 46.3 s for the 3.05 m (10 ft) clearance case.

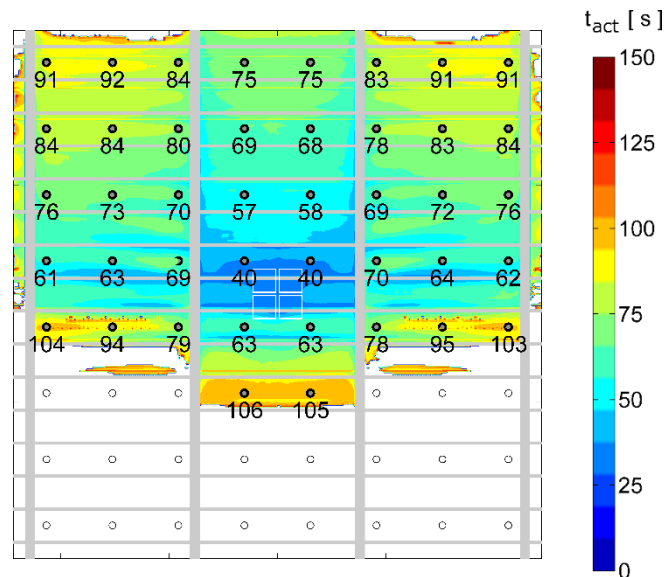


Figure 3-10: Activation of QR/OT sprinklers located 0.33 m (13 in.) below a ceiling inclined at 18.4° with its midpoint 6.1 m (20 ft) above the CUP array when purlin depth is 0.3 m (12 in.).

3.2 Ceiling Flows in the Presence of Ridges

3.2.1 Ceiling Jet Development

Following the approach in Section 3.1, flows below ceilings inclined at 18.4° with ridges located 6.1 m (20 ft) and 12.2 m (40 ft) from the ceiling mid-point were simulated. When a ridge is present on a smooth sloped ceiling, as shown in Figures 3-11 and 3-12, the initial ceiling jet development

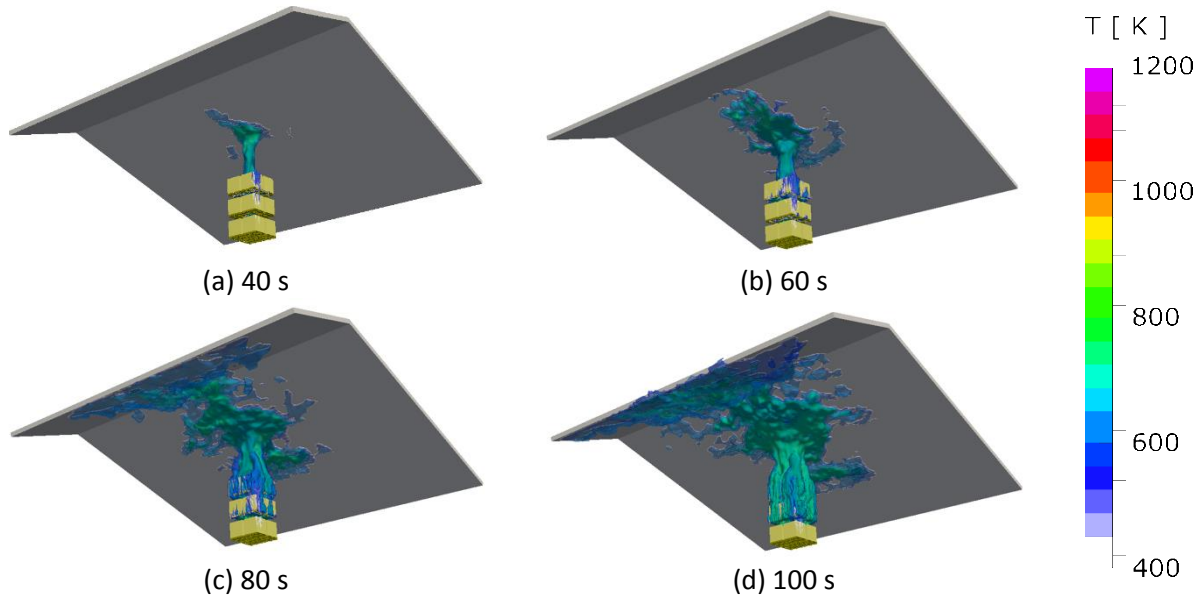


Figure 3-11: Computed CO₂ mass fraction contours colored by temperature below a 24 m x 24 m (80 ft x 80 ft) smooth ceiling inclined at 18.4° with a ridge located 6.1 m (20 ft) from the CUP array. CO₂ mass fractions in the range of 0.02-0.04 are used. Ceiling is located 3.05 m (10 ft) above the CUP array.

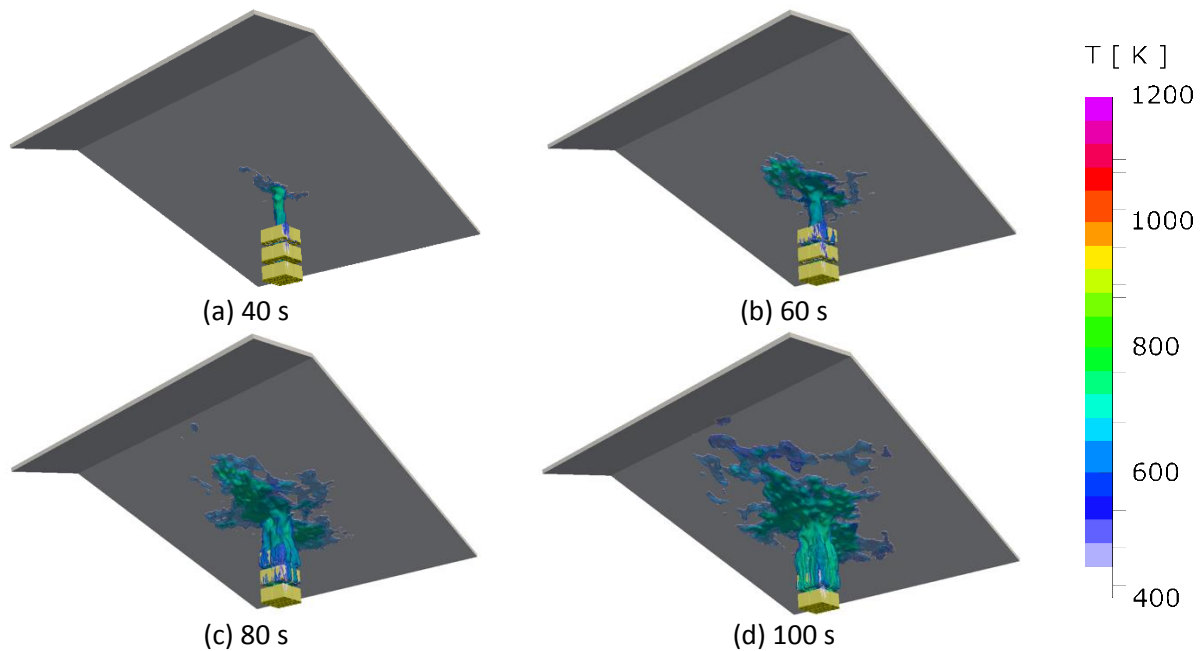


Figure 3-12: Computed CO₂ mass fraction contours colored by temperature below a 24 m x 24 m (80 ft x 80 ft) smooth ceiling inclined at 18.4° with a ridge located 12.2 m (40 ft) from the CUP array. Ceiling is located 3.05 m (10 ft) above the CUP array.

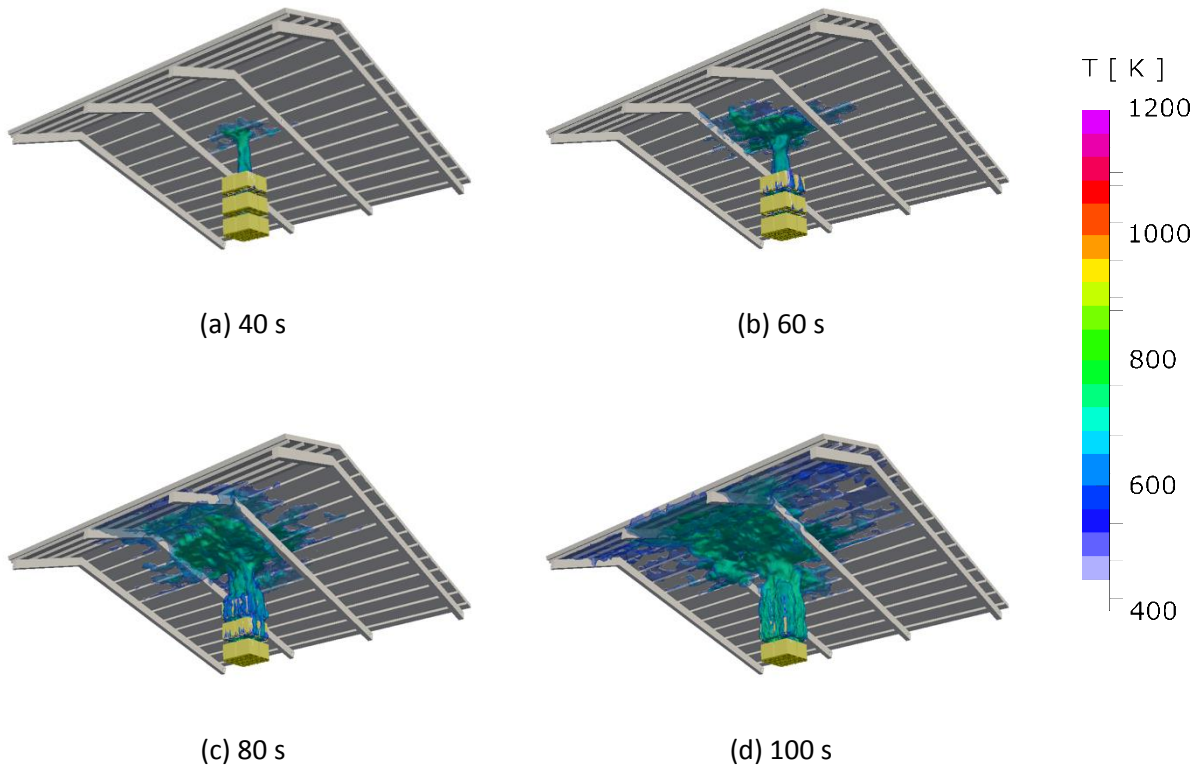


Figure 3-13: Computed CO₂ mass fraction contours colored by temperature below a 24 m x 24 m (80 ft x 80 ft) obstructed ceiling inclined at 18.4° with a ridge located 6.1 m (20 ft) from the CUP array. Ceiling is located 3.05 m (10 ft) above the CUP array. Purlins of depth 0.2 m (8 in.) and 0.6 m (24 in.) deep girders present.

(i.e., the first 60 s) is not affected by the ridge distance from the ceiling mid-point. After 60 s the ceiling jet development differs for the two ridge locations. For a ridge located 12.2 m (40 ft) from the CUP array, the ceiling jet at > 80 s (Figure 3-12(c-d)) is similar to that of the smooth ceiling in the absence of the ridge. For a ceiling with a ridge located 6.1 m (20 ft) from the CUP array, the ceiling jet at 80 s extends past the ridge, and down the slope of the ceiling on the far side of the ridge. The ceiling jet also widens significantly and the combustion products accumulate at the ridge.

Figure 3-13 shows the ceiling jet development with a ridge located 6.1 m (20 ft) from the CUP array and in the presence of obstructed construction in the form of 0.2 m (8 in.) deep purlins and 0.6 m (24 in.) deep girders. The ceiling jet prior to 80 s is not affected by the presence of the ridge when obstructed construction is present. At later times (beyond 100 s), the ridge causes the ceiling jet to extend laterally to the adjacent channels formed by the girders.

3.2.2 Activation of Quick-Response, Ordinary Temperature Sprinklers

Activation times and patterns are presented below for ceilings containing ridges. Smooth ceilings and obstructed ceiling construction features (purlins and girders) are considered in the simulations. The

activation time contours, unless explicitly mentioned, are for a plane parallel to and located 0.33 m (13 in.) below the ceiling.

3.2.2.1 Inclined Ceiling (9.5°)

The sprinkler activation patterns for a smooth ceiling inclined at 9.5° with ridges located 6.1 m (20 ft) and 12.2 m (40 ft) from the CUP array are shown in Figure 3-14(a) and (b), respectively. The ridge is represented by the thick horizontal dashed lines. Sprinkler activation patterns are not greatly affected due to the presence of the ridge. However, for the case when the ridge is 6.1 m (20 ft) from the ceiling mid-point, sprinklers near the ridge activate earlier compared to the sprinklers nearest to the ignition location. In general, the activation times on the near side of the ridge decrease by a few seconds. The average activation time for the four sprinklers closest to the CUP array, however, was within 6-7 s of the average activation time in the absence of the ridge.

For the ridge located at 6.1 m (20 ft), the sprinkler activation pattern widened on the far side of the ridge due to the accumulation of the hot fire products. This resulted in activations occurring on the far side of the ridge at approximately the same time as activations occurring on the near side of the ridge. When the ridge was located 12.2 m (40 ft) from the CUP array, the sprinkler activation times and pattern did not change significantly near the ridge unlike the 6.1 m (20 ft) case.

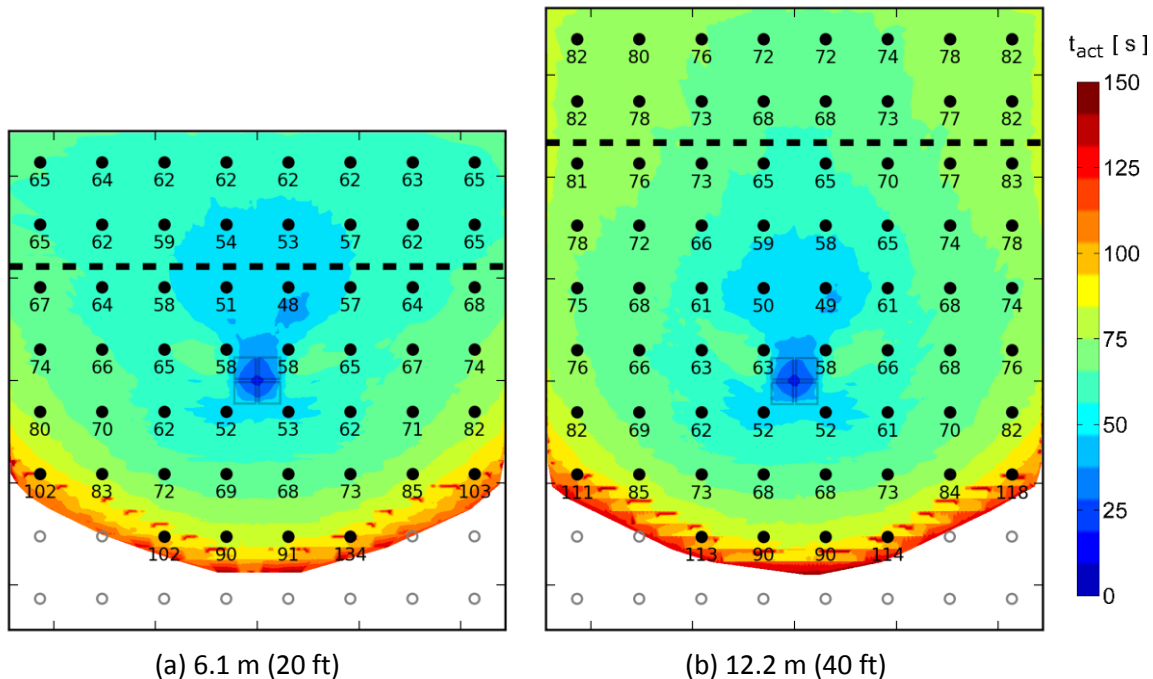


Figure 3-14: Activation time contours of QR/OT sprinklers located 0.33 m (13 in.) below a smooth ceiling inclined at 9.5° with a ridge located (a) 6.1 m (20 ft), and (b) 12.2 m (40 ft) from the CUP array. Ceiling is 3.05 m (10 ft) above the CUP array.

3.2.2.2 Inclined Ceiling (18.4°)

The activation patterns for a smooth ceiling inclined at 18.4° with ridges located 6.1 m (20 ft) and 12.2 m (40 ft) from the CUP array are shown in Figure 3-15(a) and (b), respectively. Overall, the presence of a ridge 12.2 m (40 ft) from the CUP array has a minimal effect on the sprinkler activation patterns compared to when the ridge is not present. When the ridge is located at 6.1 m (20 ft), the average activation time for the four sprinklers closest to the CUP array changed by approximately 5 s compared to the unbounded ceiling case. However, the sprinklers near the ridge activated earlier than the four sprinklers surrounding the ignition location. For the ceiling with the ridge 12.2 m (40 ft) from the CUP array, the sprinkler activation pattern does not widen as dramatically as with the ridge located 6.1 m (20 ft) from the CUP array. The activation pattern and times are also not affected significantly.

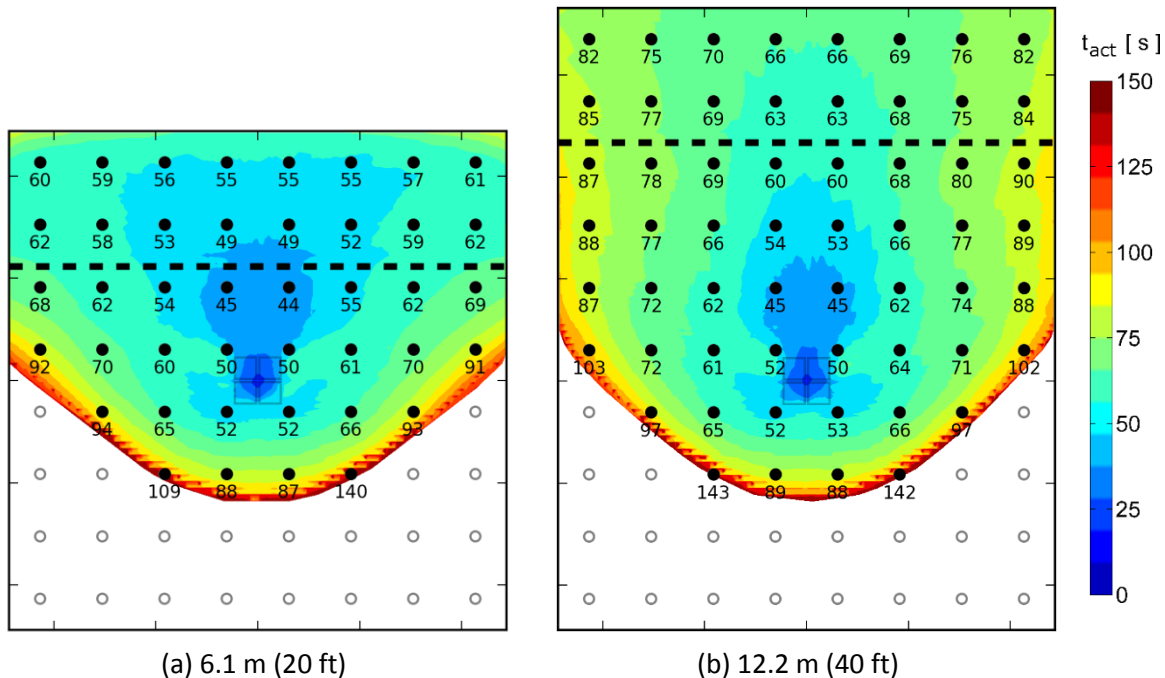


Figure 3-15: Activation time contours of QR/OT sprinklers located 0.33 m (13 in.) below a smooth ceiling inclined at 18.4° with a ridge located (a) 6.1 m (20 ft), and (b) 12.2 m (40 ft) from the CUP array. Ceiling is 3.05 m (10 ft) above the CUP array.

To examine the effect of changes in sprinkler link stand-off distance on activation time when the ridge is present, activations at distances of 0.15 m (6 in.) and 0.33 m (13 in.) are compared. Figure 3-16. shows the sprinkler activation patterns for a stand-off distance of 0.15 m (6 in.) with a smooth ceiling inclined at 18.4° and ridges located 6.1 m (20 ft) and 12.2 m (40 ft) from the CUP array. For both ridge locations, the 0.15 m (6 in.) stand-off distance generally results in less skewness of the sprinkler activation pattern toward the elevated side of the ceiling and expectedly shows earlier sprinkler activations than for the 0.33 m (13 in.) stand-off distance, particularly for sprinklers near the ignition location. For the reduced

stand-off distance, the effect of the ridge on activation times is greatly reduced and the earliest activations occur near the ignition region.

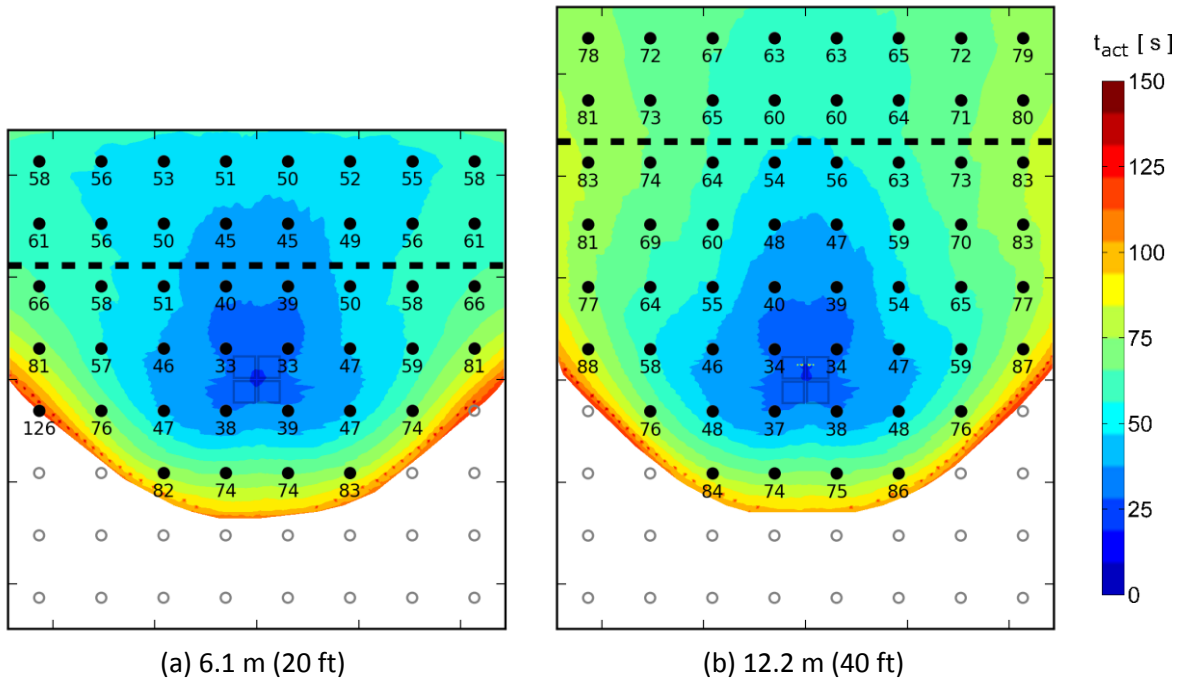


Figure 3-16: Activation time contours of QR/OT sprinklers located 0.15 m (6 in.) below a smooth ceiling inclined at 18.4° with a ridge located (a) 6.1 m (20 ft), and (b) 12.2 m (40 ft) from the CUP array. Ceiling is 3.05 m (10 ft) above the CUP array.

The combined effects of obstructed ceiling construction and a ridge located at 6.1 m (20 ft) from the ceiling mid-point on the sprinkler activation patterns are shown in Figure 3-17. The ceiling is inclined at 18.4° . Obstructed ceiling construction in the form of 0.6 m (24 in.) deep girders and 0.2 m (8 in.) deep purlins are considered. Overall, the sprinkler activation pattern in Figure 3-17 is similar to that of the obstructed ceiling inclined at 18.4° in the absence of the ridge. The average activation time of the four sprinklers closest to the ignition location remains approximately the same as for the case with the ceiling without a ridge. The first six activations occur within the central channel formed by the girders on the near side of the slope. These same six sprinklers activate first for the obstructed ceiling without the ridge. Overall, the presence of the ridge at 6.1 m (20 ft) results in a similar activation pattern as the case without the ridge.

3.2.2.3 Comparison of Smooth, Inclined Ceiling Activation Times

The presence of the ridge causes the activation time of the four sprinklers surrounding the ignition location to marginally increase (<6 s). This may be due to the local flow being affected by the presence of the ridge. The predominant effect of the ridge is the earlier activations observed for sprinklers located adjacent to the ridge, especially when the ridge is located 6.1 m (20 ft) from the ceiling mid-point. To compare the combined effect of ridge distance and ceiling inclination on the activation performance of QR/OT sprinklers, the activation times of the row of sprinklers closest to the ridge (on the near side of

the ridge) are considered. In Table 3-2, the average activation times are reported for smooth, inclined ceilings with different ridge distances. The presence of ridges causes average activation times for the eight elevated sprinklers on the near side of the ridge to reduce by 2-8 s, as shown in Table 3-2. If only the central four sprinklers near the ridge are considered, the difference in average activation times reduces to 1-3 s. Overall, the effect of the ridge on activation times is, therefore, not significant. In the presence of obstructed ceiling construction, the effect of the ridge is further reduced.

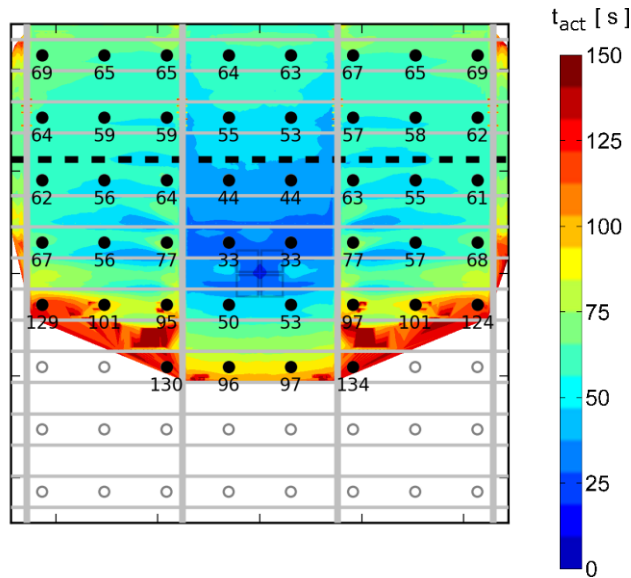


Figure 3-17: Activation time contours of QR/OT sprinklers located 0.33 m (13 in.) below an obstructed ceiling inclined at 18.4° with a ridge located 6.1 m (20 ft) from the CUP array. Ceiling is 3.05 m (10 ft) above the CUP array.

Table 3-2: Average activation times for the row of sprinklers on the near side of the ridge compared to sprinklers at the same location for the no-ridge case.

Inclination (°)	9.5		18.4	
	20 ft	40 ft	20 ft	40 ft
No Ridge	59	70	62	73
Ridge	57	74	54	69

3.2.3 Activations of Standard-Response, High Temperature Sprinklers

SR/HT activation times and patterns for a ceiling inclination of 18.4° with ridges located at 6.1 m (20 ft) and 12.2 m (40 ft) are shown in Figure 3-18. Compared to the QR/OT sprinklers, the region where SR/HT sprinklers will activate shrinks, particularly for the 12.2 m (40 ft) ridge case. In Figure 3-18(a), the activation pattern shows considerable widening on the far side of the ridge located 6.1 m (20 ft) from the CUP array. However, the average activation time of the four sprinklers near the ignition location with a ridge present is within ~2 s in absence of the ridge.

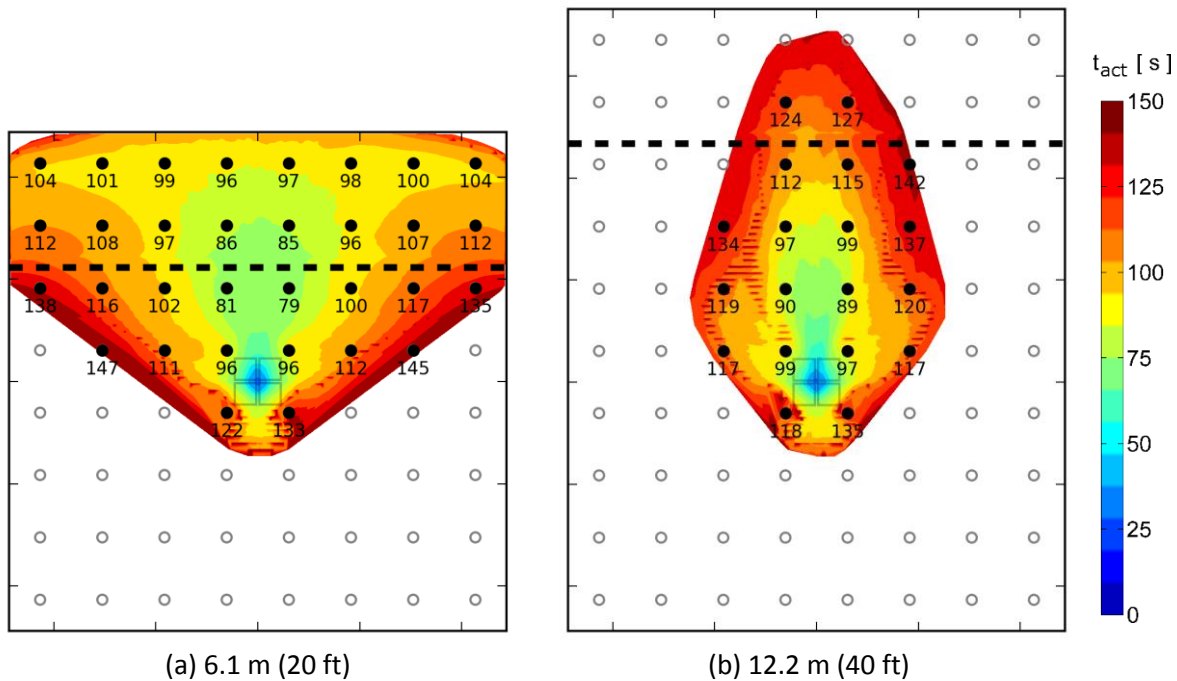


Figure 3-18: Activation time contours of SR/HT sprinklers located 0.33 m (13 in.) below a smooth ceiling inclined at 18.4° with a ridge located (a) 6.1 m (20 ft), and (b) 12.2 m (40 ft) from the CUP array. Ceiling is 3.05 m (10 ft) above the CUP array.

3.3 Summary

Based on the activation simulations involving QR/OT sprinklers, the results show that:

- For horizontal ceilings (0°) and purlin depths of up to 0.6 m (24 in.), a marginal increase (maximum 4 s) in the average activation time is observed for the four sprinklers immediately adjacent to the fire source.
- For a ceiling inclination of 9.5° and purlin depths of up to 0.3 m (12 in.), the average activation time for the four sprinklers immediately adjacent to the fire source is similar to that of the case of horizontal ceilings for the same purlin depths. The average activation times are also comparable to those of the 9.5° smooth ceiling. For a purlin depth of 0.6 m (24 in.), considerable activation delay is observed for the non-elevated sprinklers when compared to the average activation time for a smooth, horizontal ceiling. This delay may adversely impact suppression performance.
- For a ceiling inclination of 18.4° and purlin depths of up to 0.1 m (4 in.), the average activation time compares favorably with the smooth ceiling results. For purlin depths of 0.2 m (8 in.) and larger, considerable delays in non-elevated sprinkler activations are also observed which may affect suppression effectiveness.

- The presence of a ridge marginally affects the activation times of the four sprinklers surrounding the ignition location. Activations near the ridge are also affected with slightly earlier activation times observed on the near ends of the ridge.
- In the presence of the ridge, less skewness of the sprinkler activation pattern towards the elevated side of the ceiling is also observed for reduced sprinkler stand-off distance.

For SR/HT sprinklers, the following observations are made:

- At inclination angles $\geq 9.5^\circ$ and a purlin depth of 0.3 m (12 in.), highly skewed activation patterns are observed between the elevated and non-elevated sides. As sprinklers on the non-elevated side do not activate, suppression effectiveness will reduce.
- For an inclined ceiling with the ridge located 6.1 m (20 ft) from the CUP array, significantly more SR/HT sprinklers activate near the ridge compared to a ceiling in absence of a ridge. The effect of the ceiling ridge on the sprinkler activation patterns appears more significant for SR/HT than for QR/OT sprinklers.

4. Sprinkler Sprays Study

Extending the spray investigation conducted in Phase 1 [1], the effect of ceiling slope and deflector orientation (deflector parallel to the floor or to the ceiling) is further studied using sprinkler spray simulations. In the Phase 1 study, a single pendent sprinkler (K200) was used whereas in the current study two additional sprinklers, an upright sprinkler (K160) and a higher K-factor pendent sprinkler (K240), are included. The K240 sprinkler is included as it is commonly used in the industry. With the addition of these two sprinklers, the most common sprinkler occurrences in warehouse storage have now been considered.

The two representative scenarios investigated earlier [1] are again considered in this study: when a single sprinkler activates above the CUP rack-storage array and when four sprinklers operate together. The ceiling clearance for the spray calculations is 3.05 m (10 ft) from the top of the CUP array to the ceiling midpoint.

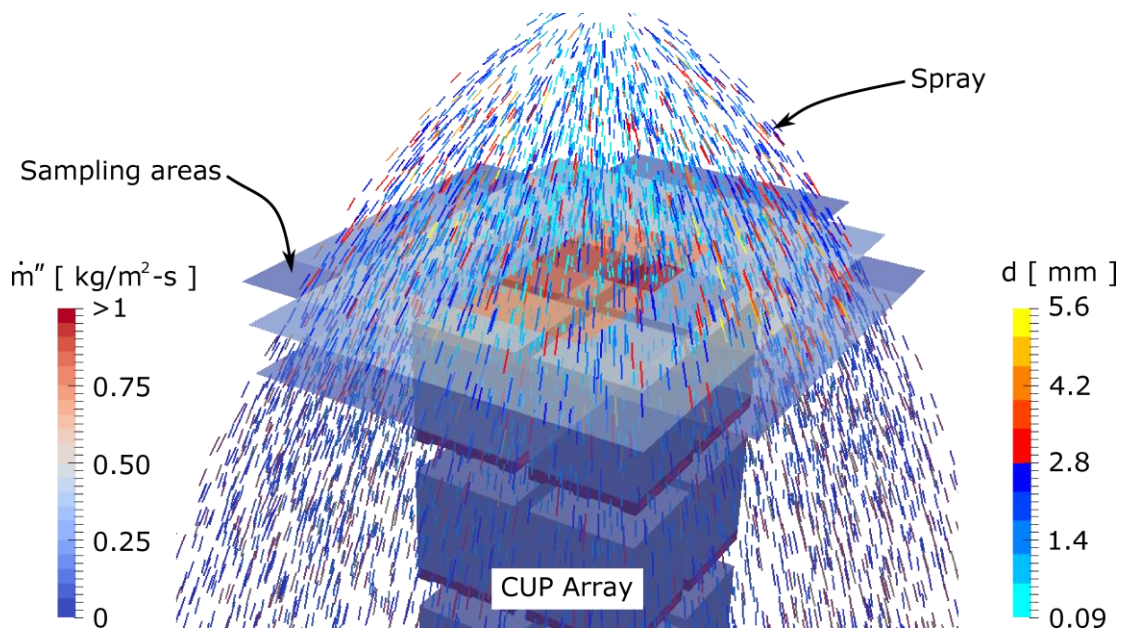


Figure 4-1: Spray from an upright K160 sprinkler and the CUP array. The 0.61 m x 0.61 m (2 ft x 2 ft) sampling areas are also shown.

Comparisons of simulated water flux with two different sprinkler orientations are made for both a cold-flow case and when the fire plume is present. For each case, spray calculations are conducted for a duration of 30 s and the collected water-flux distribution 0.3 m (1 ft) above the CUP array is averaged for the last 20 s of the simulations. The water flux is recorded at an array of 0.61 m x 0.61 m (2 ft x 2 ft) sampling areas covering a total area of ~149 m² (1600 ft²). Figure 4-1 shows the spray originating from a single upright K160 sprinkler engulfing the CUP array. The sampling areas are shown above the array. Comparison is also made between cases by integrating the water flow rate for a 3.05 m x 3.05 m (10 ft x 10 ft) area located 0.3 m (1 ft) above the CUP array. This area covers the region where fire

growth is taking place and where pre-wetting is required to successfully control further lateral spread to neighboring storage arrays.

4.1 Sprinkler Operating Conditions and Ceiling Inclination Selection

The flow rate from each sprinkler is kept approximately equal to 370 lpm (99 gpm), the same as the K200 pendent sprinkler at 3.4 bar (50 psi) used in the previous study [1]. Thus, the upright K160 sprinkler is simulated at 5.2 bar (75 psi) and the pendent K240 sprinkler is simulated at 2.4 bar (35 psi). Two ceiling inclinations are considered in this study: 0° and 18.4°. An inclination of 33.7° was also considered in the previous study [1] where it was found that such high inclination angles adversely impact the spray density on the fire because of a highly-skewed activation pattern (first four activations occur on the elevated ceiling side). In this study, therefore, the ceiling inclination of 33.7° is not included.

4.2 Selection of Heat Release Rates

For the single- and four-sprinkler simulations, the plume strength is kept fixed by the selection of a constant convective HRR. Comparison of collected water flux above the CUP array are made for the two inclination cases (0° and 18.4°). For the one-sprinkler case, the activation time of the QR/OT sprinkler is found to be approximately 25 s irrespective of the ceiling orientation. The convective HRR at 25 s is approximately 600 kW. The fire convective HRR is therefore kept constant at 600 kW for the single sprinkler spray calculations.

For the other set of simulations, the four sprinklers surrounding the CUP array are selected for the spray calculations. In the case of the horizontal ceiling, the first four sprinklers to activate are located around the CUP array. For the 18.4° case, only minor time differences exist between the first four sprinklers surrounding ignition and the four sprinklers on the elevated side. A constant convective HRR of 2.6 MW is used in these simulations. A detailed description of the HRR selection process is available in Section 4.2 and Table 4-1 of Ref. [1].

4.3 Upright K160 Sprinkler

4.3.1 *Water-flux Distributions from One Sprinkler*

In the case of the horizontal ceiling, the sprinkler deflector is always parallel to the floor and the spray from the upright K160 is distributed around the rack-storage array. An instantaneous snapshot of the sprinkler spray for the 0° inclination case is shown in Figure 4-2(a). The 600-kW convective-HRR fire is also shown inside the rack-storage array.

Figure 4-2(b) shows the spray distribution when the ceiling is inclined at 18.4° and for the parallel-to-floor deflector orientation. The spray distribution remains almost identical to the horizontal-ceiling case, except for an asymmetric distribution of the smallest droplets that are entrained in the ceiling jet and are present primarily on the elevated ceiling side. With the ceiling at 18.4° and the parallel-to-ceiling

deflector orientation, a significant portion of the spray tends to deposit water on the elevated ceiling side and an asymmetric spray distribution can be observed in Figure 4-2(c).

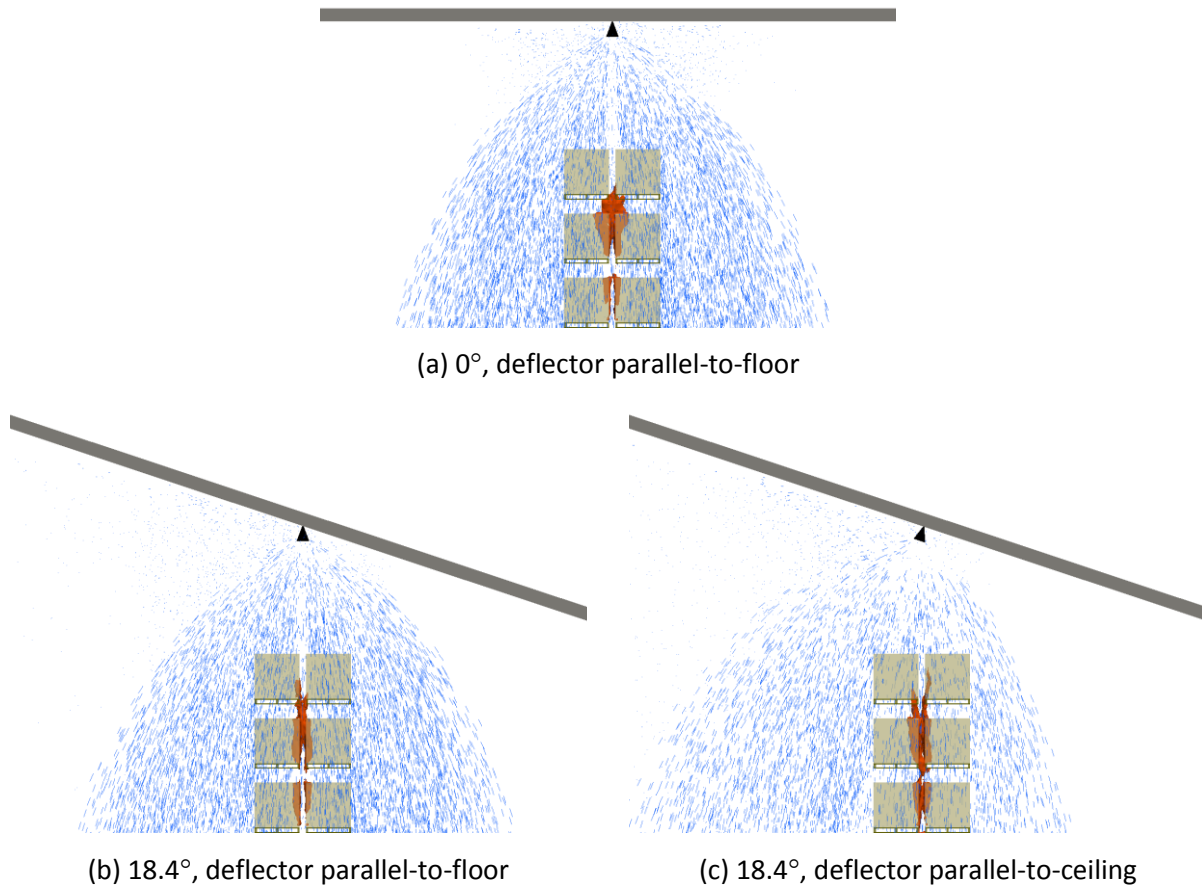


Figure 4-2: Instantaneous snapshots of sprays originating from the upright K160 sprinkler for (a) 0° inclination, deflector parallel to floor, (b) 18.4° inclination, deflector parallel-to-floor, and (c) 18.4° inclination, deflector parallel-to-ceiling. The 600-kW convective-HRR fire is shown by the instantaneous contour of the stoichiometric mixture fraction inside the rack-storage array.

The water-flux distributions at a collection plane 0.3 m (1 ft) above the rack-storage array are presented below. For the horizontal ceiling, when no fire is present, Figure 4-3(a) shows the distribution for the upright K160 sprinkler with mass flux of $\sim 1.4 \text{ kg/m}^2\text{-s}$ present in the central region. Mass fluxes of the order of $0.75 \text{ kg/m}^2\text{-s}$ are observed above and below the central region. Lower fluxes are present on the left and right sides. The lower fluxes are because the sprinkler arm is oriented in the x-direction. Comparatively, for the pendent K200 sprinkler, the water-flux distribution area is larger [1]. The larger area is due to the fact that, for the same flow rate, storage-type pendent sprinklers have wider spray distribution patterns compared to upright sprinklers. In the presence of the 600-kW fire, the distribution is affected above the rack-storage array compared with the pendent K200 sprinkler performance [1]. For

the horizontal ceiling case, the water-flux distribution shows maximum values on the order of $0.5 \text{ kg/m}^2\text{-s}$, which is considerably lower than the $>1 \text{ kg/m}^2\text{-s}$ when no fire is present. Unlike the pendent K200 sprinkler [1], the upright K160 sprinkler lacks a central core consisting of high momentum droplets and, therefore, even a lower strength plume of 600-kW affects the water-flux distribution above the ignition location.

When the ceiling is inclined at 18.4° and the sprinkler deflectors are kept parallel-to-floor, the water-flux distribution is not affected to a large extent (see Figure 4-3(b)). The distribution is similar to the 0° case, except for skewed distributions visible above and below the central region. In presence of the fire, the water flux in the central region reduces and the plume entrains the droplets. The fire plume also inhibits and evaporates the droplets. The water-flux distribution remains similar to the horizontal ceiling case. The movement of the smaller droplets outwards from the ignition region is also observed in the water-flux distribution of the pendent K200 sprinkler [1].

For the case of the 18.4° ceiling inclination and deflector parallel-to-ceiling, the water-flux distribution shows skewness toward the elevated ceiling side, causing a marked reduction in the coverage area in the non-elevated ceiling side adjacent to the ignition location. Figure 4-3(c) shows that the mass flux values on top of the rack-storage array are comparable to the case with deflector parallel-to-floor. In contrast, for the pendent K200 sprinkler, greater skewness in the distribution was observed on the elevated ceiling side [1]. When the fire is present, the mass flux distribution above the rack-storage array is significantly affected. The distribution in the presence of the fire plume also skews towards the elevated ceiling side and mass fluxes of $\sim 0.4 \text{ kg/m}^2\text{-s}$ are observed further away from the rack-storage array. In comparison to the deflector parallel-to-floor case, an overall reduction of water flux above the rack-storage array is observed.

In summary, from the results reported above, it can be said that for sloped ceilings the deflector orientation affects the mass flux results for the upright K160 sprinkler. In the presence of the relatively weak 600-kW fire plume, the deflector parallel-to-ceiling configuration skews the water distribution toward the elevated ceiling side, which is not the case when the deflector is kept parallel-to-floor.

4.3.2 Comparison of Integrated Mass Flux

To provide a comparison between the current results for the upright K160 sprinkler and the previously generated results for the pendent K200 sprinkler [1], integrated mass flow rates over a $3.05 \text{ m} \times 3.05 \text{ m}$ ($10 \text{ ft} \times 10 \text{ ft}$) area above the rack-storage array are considered. In Figure 4-4(a), a comparison is made when no fire is present: the mass flow rate as a function of ceiling inclination is shown. The mass flow rate through the 9.3 m^2 (100 ft^2) area for the upright K160 sprinkler does not change when the ceiling inclination increases from 0° to 18.4° . This is true for both the deflector orientations of parallel-to-floor and parallel-to-ceiling. For the horizontal ceiling case, we observe that the upright K160 sprinkler at 5.2 bar (75 psi) provides $\sim 38\%$ higher flow rate through the 9.3 m^2 (100 ft^2) area as compared to the pendent K200 sprinkler at 3.4 bar (50 psi). This difference increases to $\sim 46\%$ for the 18.4° ceiling inclination.

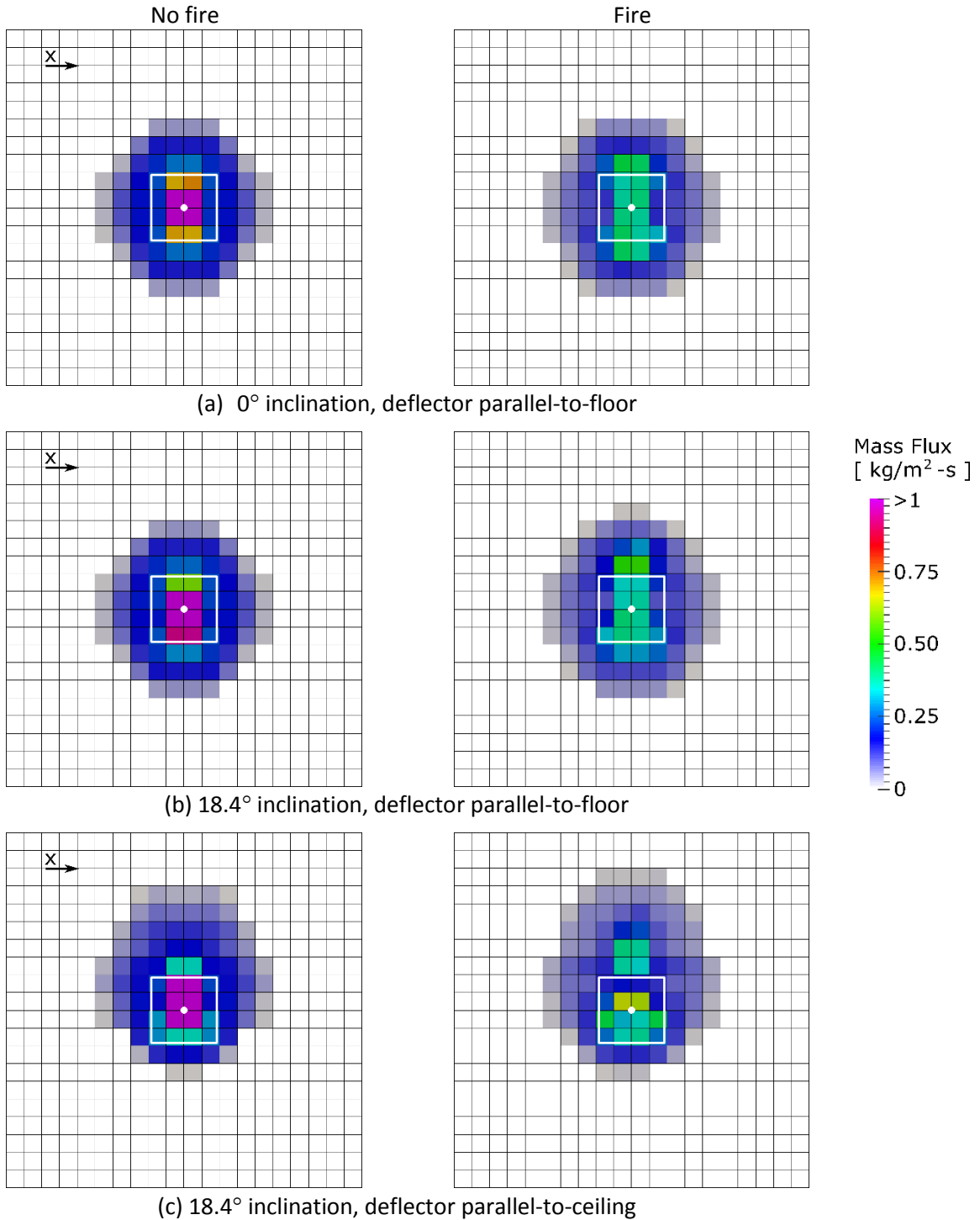
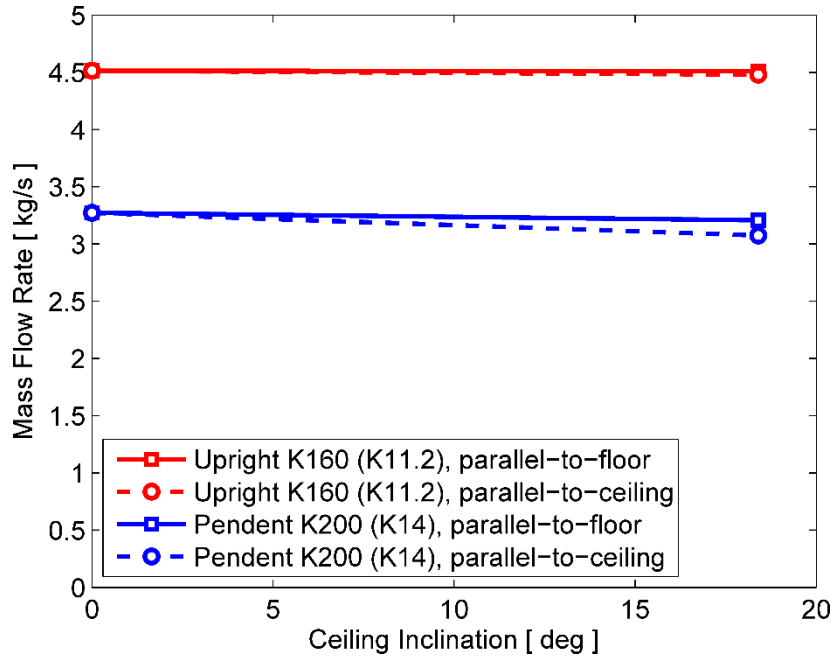
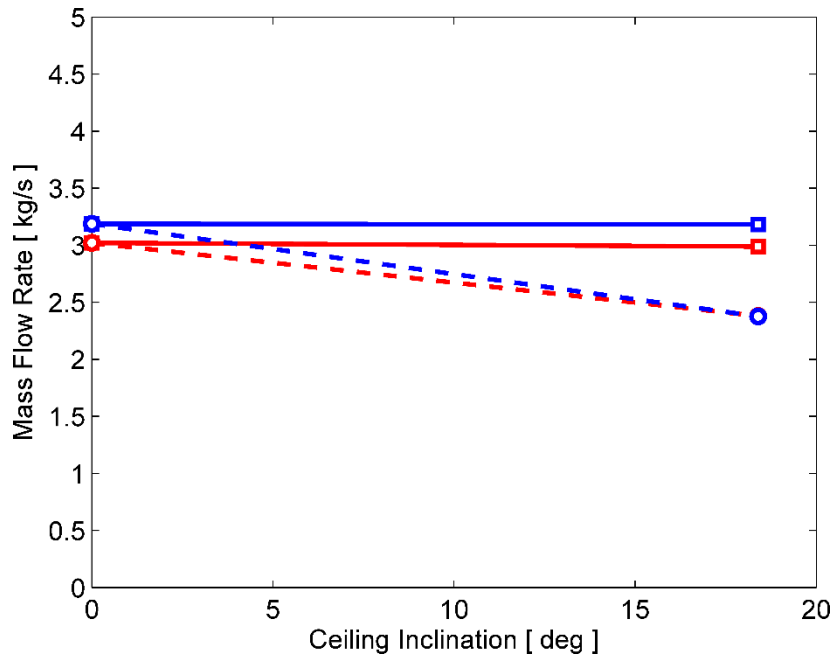


Figure 4-3: Comparison of droplet mass flux distributions shown for a single upright K160 sprinkler when no fire is present and when a 600-kW convective-HRR fire is present. The sprinkler arms are oriented in the x-direction.



(a) No fire



(b) Fire

Figure 4-4: Time-averaged droplet mass flow rate through a 3.05 m x 3.05 m (10 ft x 10 ft) sampling area surrounding the ignition location at a height of 0.3 m (1 ft) above the CUP rack-storage array as a function of ceiling inclination. A single sprinkler is located above the ignition location: (a) without fire, and (b) with a fire of constant 600-kW convective HRR. Computed mass flow rates for an upright K160 sprinkler are compared against previous results for a pendent K200 sprinkler [1].

In the presence of the 600-kW fire, the mass flow rate for the upright K160 sprinkler reduces by ~33% for the horizontal ceiling case, compared to a reduction of ~2.6% for the pendent K200 sprinkler, as seen in Figure 4-4(b). The marginal difference for the pendent K200 sprinkler is due to the stronger momentum of the spray core overcoming the plume momentum. When the ceiling inclination is 18.4° and the deflector orientation is parallel-to-floor, the mass flow rate value remains identical to the horizontal ceiling case for both the upright K160 and pendent K200 sprinklers. However, when the deflector orientation is parallel-to-ceiling, mass flow rates are reduced by ~21% and ~25% for the upright K160 and pendent K200 sprinklers, respectively. Overall, the performance of the upright K160 sprinkler is similar to that of the pendent K200 sprinkler when a single sprinkler above the ignition location activates. For both sprinklers, the deflector parallel-to-floor condition provides superior performance in the presence of the fire.

4.3.3 *Water-flux Distributions from Four Sprinklers*

The impact of ceiling inclination and deflector orientation is also studied when the fire is located among four sprinklers. In this case, the vertical distance of the sprinkler deflector from the floor varies when the ceiling is inclined.

In Figure 4-5, instantaneous snapshots of sprays originating from the upright K160 sprinklers are shown for two inclination angles (0° and 18.4°) and two orientations of the deflector (parallel to the floor or to the ceiling). The sprinklers are indicated by the black cones and the 2.6-MW fire is also shown. For the horizontal ceiling, the sprays from the four sprinklers engulf the central region where the fire is present (see Figure 4-5(a)). Inclining the ceiling at 18.4° with the deflectors parallel-to-floor, shown in Figure 4-5(b), causes two sprinklers to be elevated and two to be lower. This results in higher mass flux values below the lower sprinklers. When the ceiling is at 18.4° but the deflectors are parallel-to-ceiling, the spray pattern gets skewed with a large percentage of the spray falling further away from the fire region, as can be observed in Figure 4-5(c). However, in this scenario, the lower sprinklers provide more water directed towards the fire region as compared to when the deflectors are parallel-to-floor.

For the 0° inclination case, the maximum water flux occurs right below the individual upright K160 sprinkler locations (see Figure 4-6 (a)). Due to the presence of the 2.6-MW fire plume in the rack-storage region, the mass flux values observed are small (<0.5 kg/m²-s) compared to the regions below the sprinklers where values of ~1 kg/m²-s are observed. Compared to the upright K160 sprinkler, the water-flux distribution from the pendent K200 sprinkler covers a wider region but above the rack-storage array low mass flux values are observed [1].

When the ceiling inclination is 18.4° and the sprinkler deflectors are parallel-to-floor, a higher mass flux below the sprinklers on the lower side of the ceiling is observed than for the sprinklers on the elevated side (~1.7 kg/m²-s compared to <1.4 kg/m²-s), as shown in Figure 4-6(b). The distribution pattern for the 18.4° ceiling with deflectors parallel-to-floor is quite similar to the one for the horizontal ceiling case as shown in Figure 4-6 (a). The relatively small difference of the distribution patterns between the horizontal and the 18.4° inclined ceiling cases with the deflectors parallel-to-floor was also observed for the pendent K200 sprinkler [1].

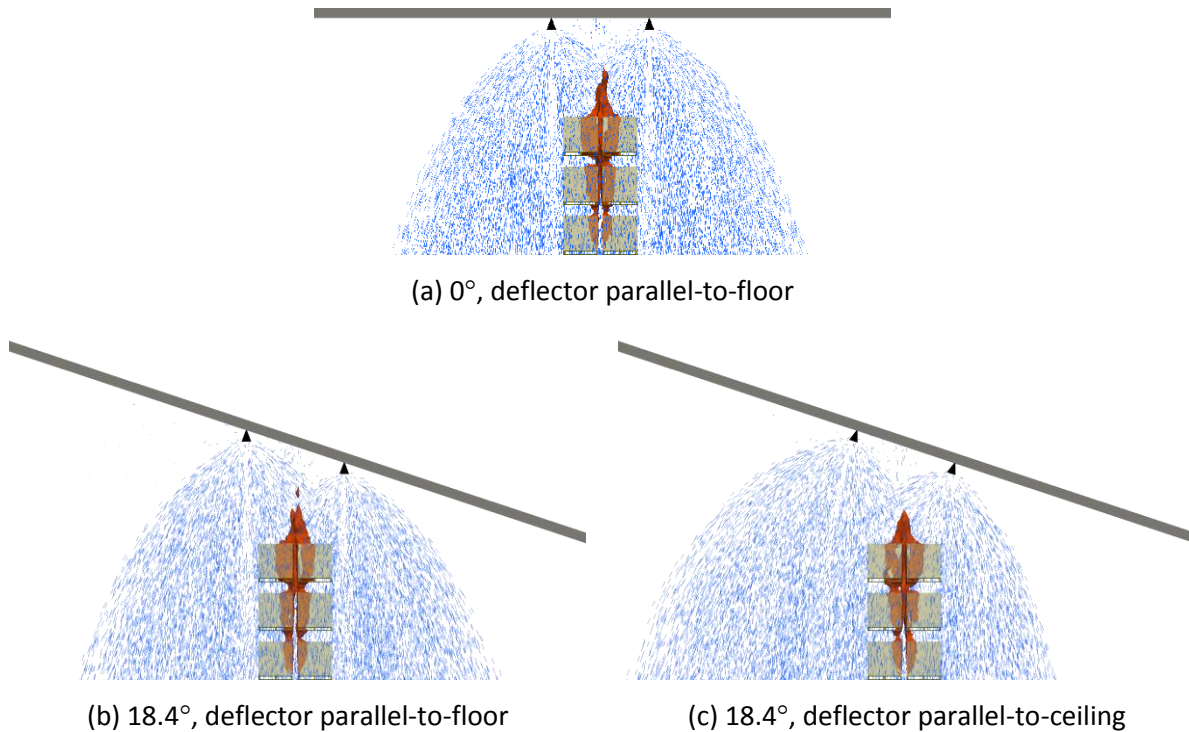


Figure 4-5: Instantaneous snapshots of sprays originating from four upright K160 sprinklers (two injection locations are visible in the images) for (a) 0° inclination, deflector parallel-to-floor, (b) 18.4° inclination, deflector parallel-to-floor, and (c) 18.4° inclination, deflector parallel-to-ceiling. The 2.6-MW convective-HRR fire is shown by the instantaneous contour of the stoichiometric mixture fraction.

For the same ceiling inclination with deflectors parallel-to-ceiling, the water-flux distribution above the rack-storage array for the upright K160 sprinklers is shown in Figure 4-6 (c). Compared to the distribution with deflectors parallel-to-floor, between 35-65% higher water flux is observed below the sprinkler locations. For the lower sprinklers, the outer spray cone which carries a larger water flux tilts toward the elevated side, therefore, increasing the water flux below the sprinkler locations. The spray from the elevated sprinklers also provides marginal increase in the water flux below the lower sprinklers. Similarly, the spray from the lower sprinklers also contributes to the increase of water flux below the elevated sprinklers. Compared to the distribution observed for the upright K160 sprinklers, the water distribution from the pendent K200 sprinklers showed higher mass flux regions moving in the direction of the ceiling slope [1].

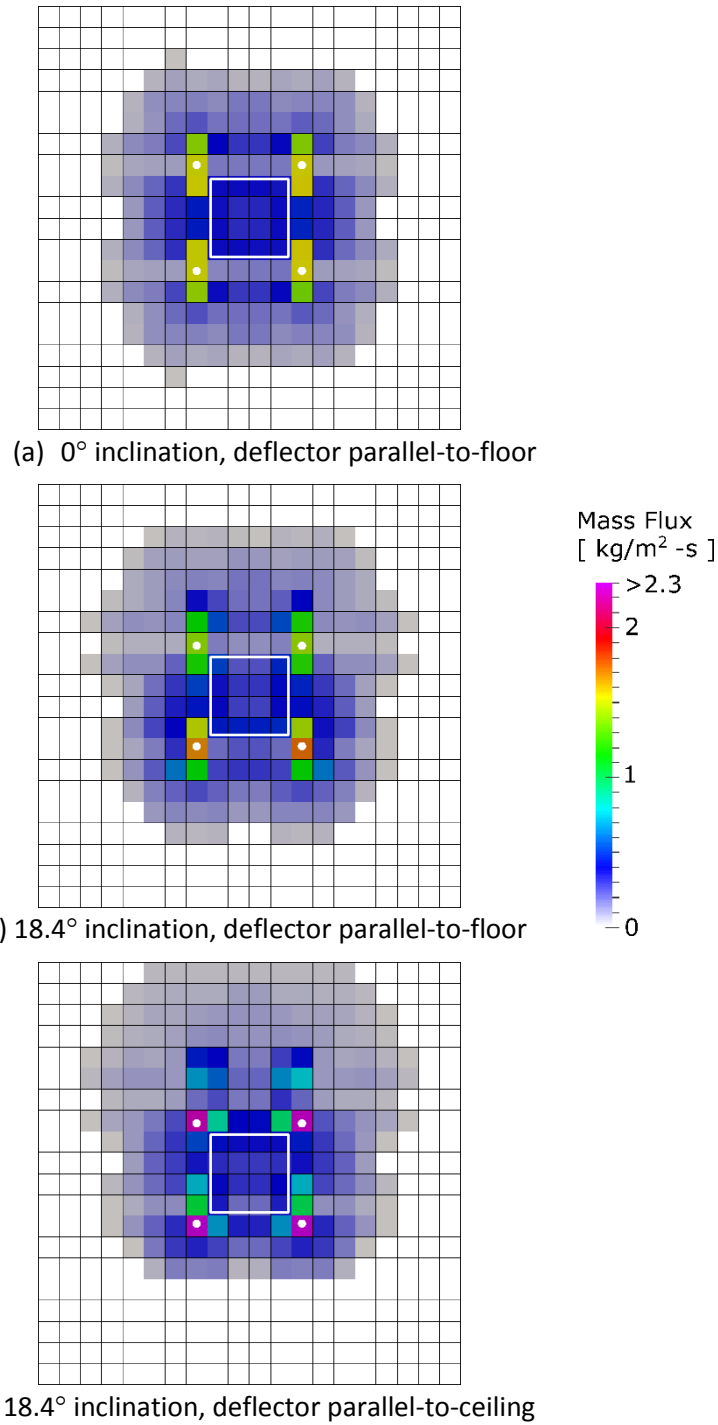


Figure 4-6: Comparison of droplet mass flux distributions shown for four upright K160 sprinklers surrounding the ignition location when a 2.6-MW convective-HRR fire is present.

4.3.4 Comparison of Integrated Mass Flux

Integrated mass flow rates through a 3.05 m x 3.05 m (10 ft x 10 ft) area 0.3 m (1 ft) above the rack-storage array are also computed for the four sprinklers case. Figure 4-7 shows a comparison between mass flow rates for the upright K160 sprinkler at 5.2 bar (75 psi) and the pendent K200 sprinkler at 3.4 bar (50 psi), when the 2.6-MW fire is present. When the ceiling is horizontal, compared to the pendent K200 sprinkler mass flow rate, the upright K160 sprinklers provide marginally higher mass flow rate over the 3.05 m x 3.05 m (10 ft x 10 ft) area. Inclining the ceiling at 18.4° and with the deflectors parallel-to-floor, the mass flow rate for the upright K160 sprinklers remains the same, whereas when the deflectors are parallel-to-ceiling, an increase of 5% is observed. A similar trend is also observed for the pendent K200 sprinklers.

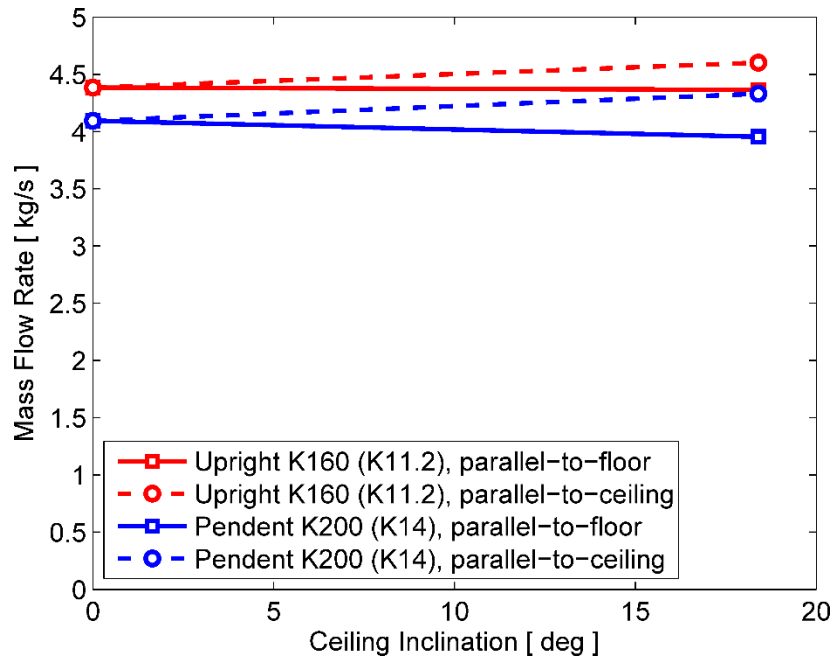


Figure 4-7: Time-averaged droplet mass flow rate through a 3.05 m x 3.05 m (10 ft x 10 ft) sampling area surrounding the ignition location at a height of 0.3 m (1 ft) above the CUP rack-storage array as a function of ceiling inclination. Four sprinklers are located below the ceiling with a fire of constant 2.6-MW convective HRR.

4.4 Pendent K240 Sprinkler

4.4.1 Water-flux Distributions from One Sprinkler

For the horizontal ceiling, the spray from the pendent K240 sprinkler falls directly on top of the rack-storage array. An instantaneous snapshot of the sprinkler spray for the 0° inclination case is shown in Figure 4-8(a). The 600-kW convective-HRR fire is also shown inside the rack-storage array.

Figure 4-8(b) shows the spray distribution when the ceiling is inclined at 18.4° and for the parallel-to-floor deflector orientation. The spray distribution remains almost identical to the horizontal-ceiling case.

With the ceiling at 18.4° and the parallel-to-ceiling deflector orientation, an asymmetric spray distribution around the rack-storage array can be observed in Figure 4-8(c). Due to the weakened spray momentum above the ignition location, the instantaneous flame height is also observed to be greater.

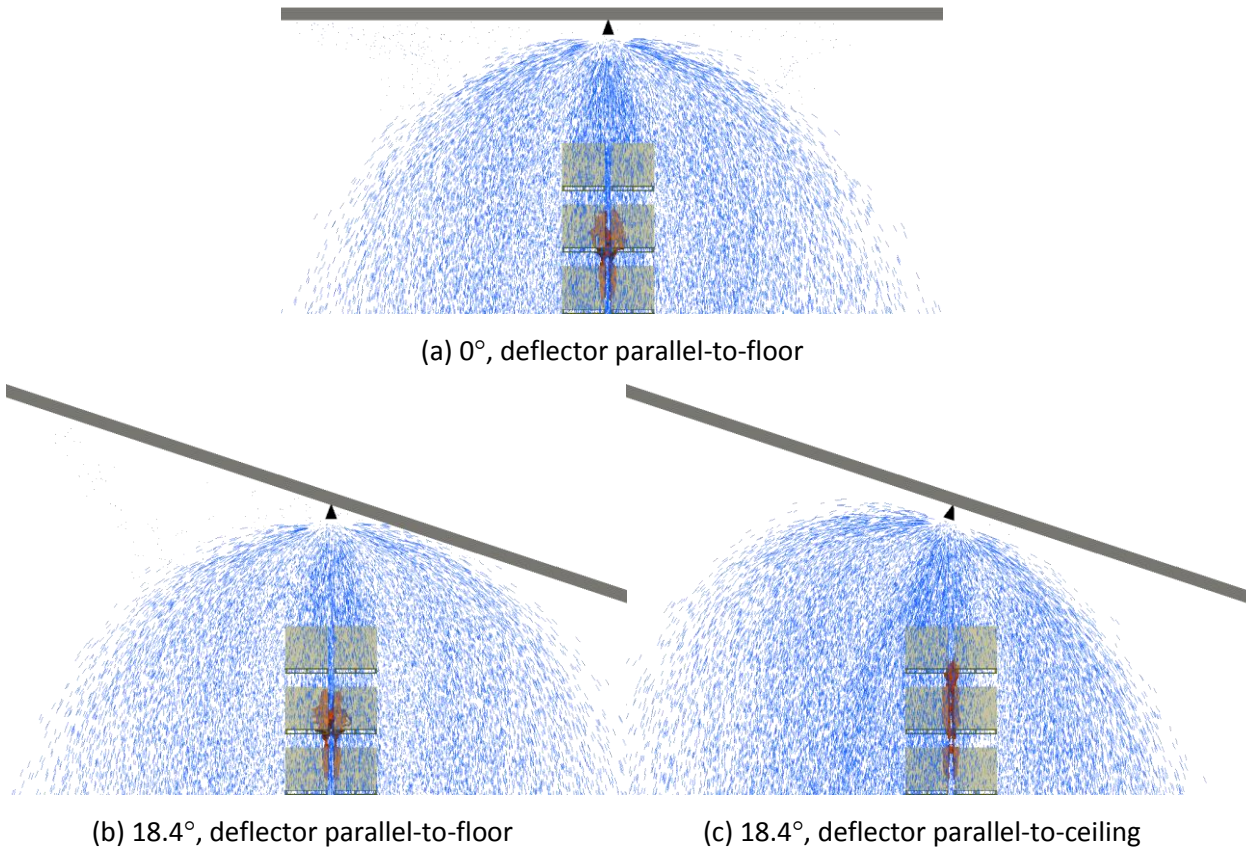


Figure 4-8: Instantaneous snapshots of sprays originating from the K240 sprinkler for (a) 0° inclination, deflector parallel to floor, (b) 18.4° inclination, deflector parallel-to-floor, and (c) 18.4° inclination, deflector parallel-to-ceiling. The 600-kW convective-HRR fire is shown by the instantaneous contour of the stoichiometric mixture fraction inside the rack-storage array.

The droplet mass flux distributions at a collection plane 0.3 m (1 ft) above the rack-storage array are presented below. For the horizontal ceiling, when no fire is present, Figure 4-9(a) shows the water-flux distribution. Maximum mass flux values of $>1.6 \text{ kg/m}^2\text{-s}$ are observed in the central region. Mass fluxes of the order of $0.5 \text{ kg/m}^2\text{-s}$ are also observed around the ignition region. Lower fluxes ($<0.25 \text{ kg/m}^2\text{-s}$) are present outside the footprint of the rack-storage array. In the presence of the 600-kW fire, to a large extent the mass flux distribution above the rack-storage array does not change significantly, as can be observed in Figure 4-9(a). This is because, similar to the K200 sprinkler, the pendent K240 sprinkler has a strong central core with higher downward momentum which overcomes the plume's upward thrust.

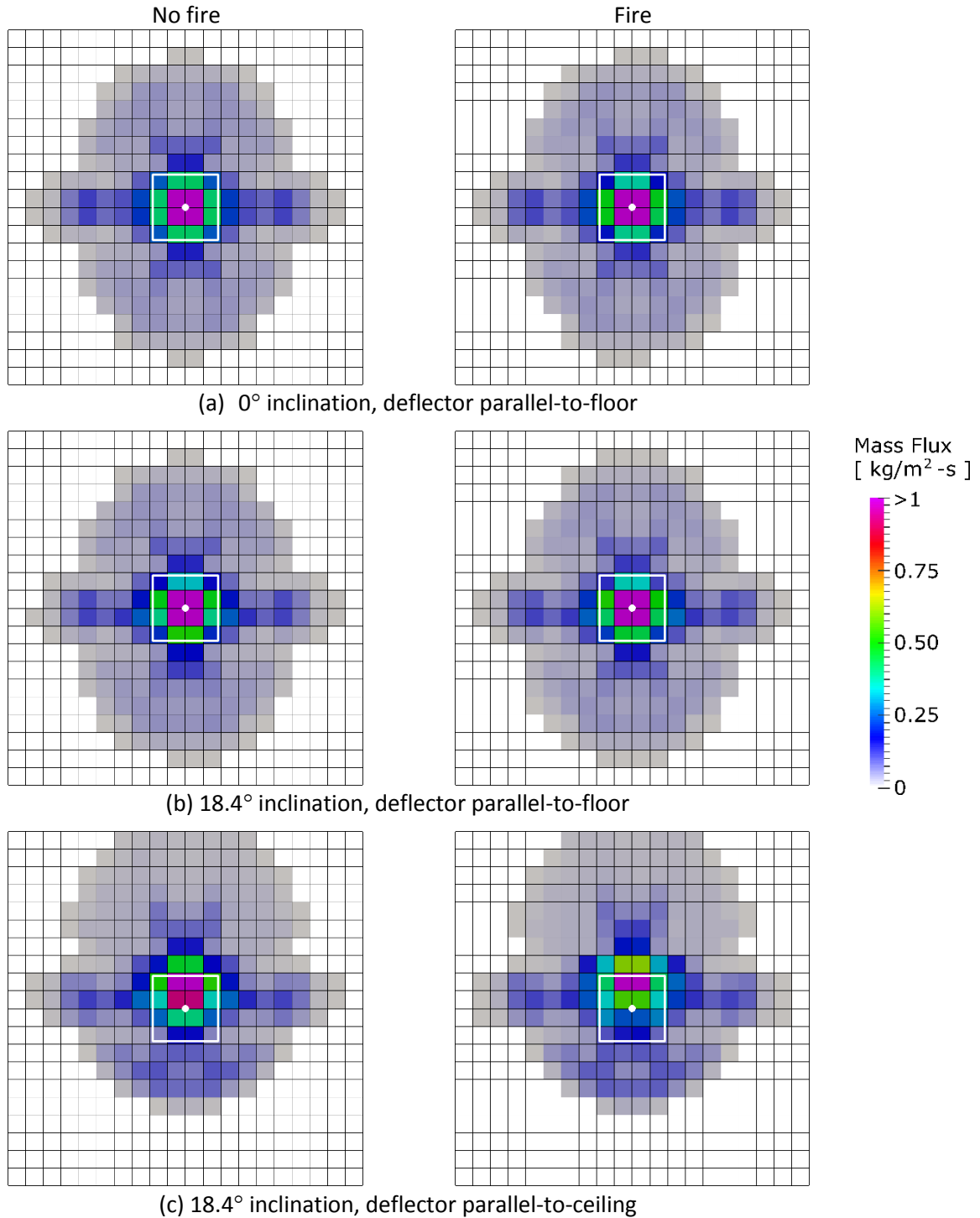


Figure 4-9: Comparison of droplet mass flux distributions shown for a single pendent K240 sprinkler when no fire is present and when a 600-kW convective-HRR fire is present. The sprinkler arm is oriented in the x-direction.

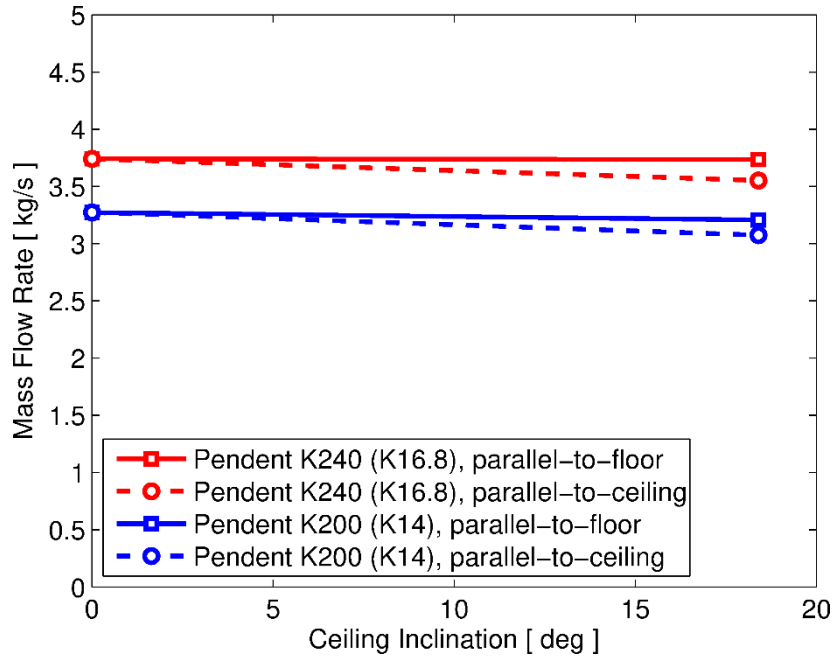
When the ceiling is inclined at 18.4° and the sprinkler deflectors are kept parallel-to-floor, the mass flux distribution is essentially not affected (see Figure 4-9(b)). The water flux on the lower side at ~ 1.8 m (6 ft) from the ignition location increases marginally due to the re-distribution of the spray impinging on the ceiling. In the presence of the fire plume, the water-flux distribution is not affected, similar to the horizontal ceiling case.

In case of the ceiling inclined at 18.4° and the sprinkler deflectors kept parallel-to-ceiling, an asymmetric water-flux distribution is observed around the ignition region (see Figure 4-9(c)). This is because the sprinkler spray tends to travel further away from the rack-storage array toward the elevated ceiling side. In the presence of the fire, a reduction of up to 50% in mass flux is observed above the ignition location compared to the peak values observed in the absence of the fire.

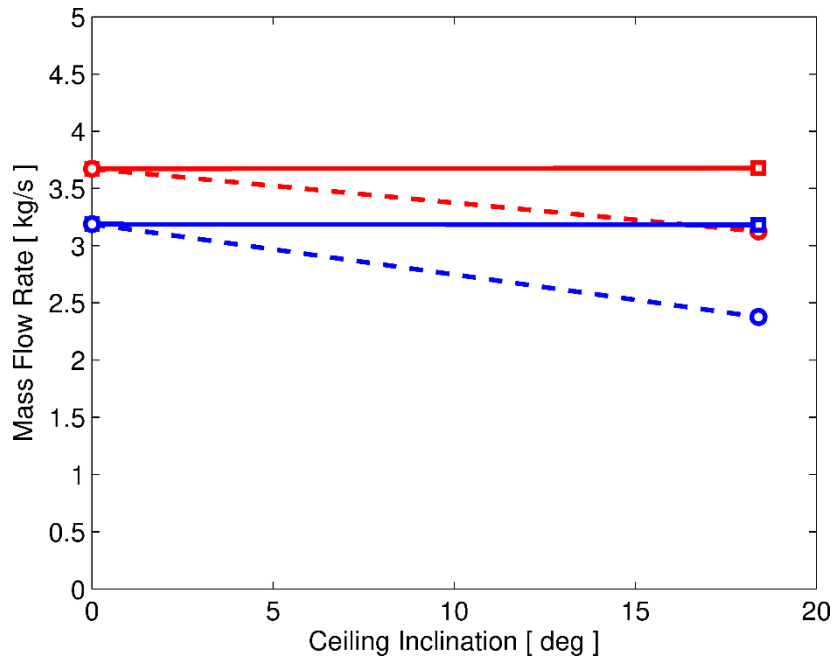
4.4.2 Comparison of Integrated Mass Flux

To provide a comparison of performance, the pendent K240 sprinkler spray distributions are plotted with the previous results of the pendent K200 sprinkler. Integrated mass flow rates through a 3.05 m x 3.05 m (10 ft x 10 ft) area above the rack-storage array are considered. In Figure 4-10(a), a comparison is made when no fire is present: the mass flow rate as a function of ceiling inclination is shown. The mass flow rate through the 9.3 m² (100 ft²) area for the K240 sprinkler does not change when the ceiling inclination increases from 0° to 18.4° for the parallel-to-floor deflector orientation. In the case of the parallel-to-ceiling orientation, a decrease of $\sim 5\%$ is observed when the ceiling inclination increases from 0° to 18.4° . A similar decrease of $\sim 6\%$ was also observed for the K200 sprinkler. The K240 sprinkler at 2.4 bar (35 psi) provides ~ 14 - 16% higher flow rate through the 9.3 m² (100 ft²) area as compared to the K200 sprinkler at 3.4 bar (50 psi) for both ceiling inclinations.

In the presence of the 600-kW fire, the mass flow rate for the K240 sprinkler reduces marginally for the horizontal ceiling case. This behavior is also observed in the case of the K200 sprinkler, as seen in Figure 4-10(b). The plume momentum is overcome by the higher momentum from the central spray core. When the ceiling inclination is 18.4° and the deflector orientation is parallel-to-floor, the mass flow rate value remains identical to the horizontal ceiling case for both the K240 and K200 sprinklers. However, when the deflector orientation is parallel-to-ceiling, mass flow rates are reduced by $\sim 15\%$ and $\sim 25\%$ for the K240 and K200 sprinklers, respectively. The deflector parallel-to-floor condition provides superior performance in the presence of the fire for both sprinklers.



(c) No fire



(d) Fire

Figure 4-10: Time-averaged droplet mass flow rate through a 3.05 m x 3.05 m (10 ft x 10 ft) sampling area surrounding the ignition location at a height of 0.3 m (1 ft) above the CUP rack-storage array as a function of ceiling inclination. A single sprinkler is located above the ignition location: (a) without fire, and (b) with a fire of constant 600-kW convective HRR. Computed mass flow rates for a pendent K240 sprinkler are compared against previous results for a pendent K200 sprinkler.

4.4.3 Water-flux Distributions from Four Sprinklers

In Figure 4-11, instantaneous snapshots of sprays originating from four pendent K240 sprinklers are shown for two inclination angles (0° and 18.4°) and two orientations of the deflector (parallel to the floor or to the ceiling). The sprinklers are indicated by the black cones and the 2.6-MW fire is also shown. For the horizontal ceiling, the spray from the four sprinklers falls primarily around the central fire region (see Figure 4-11(a)). Inclining the ceiling at 18.4° with the deflectors parallel-to-floor, shown in Figure 4-11(b), does not affect the spray distribution considerably. When the ceiling is at 18.4° and the deflectors are parallel-to-ceiling, the spray pattern gets skewed with a large percentage of the drops falling further away from the fire region, as can be observed in Figure 4-11(c). However, as in the case of the upright K160 and the pendent K200 sprinklers, the lower sprinklers provide more water directed toward the fire region as compared to when the deflectors are parallel-to-floor.

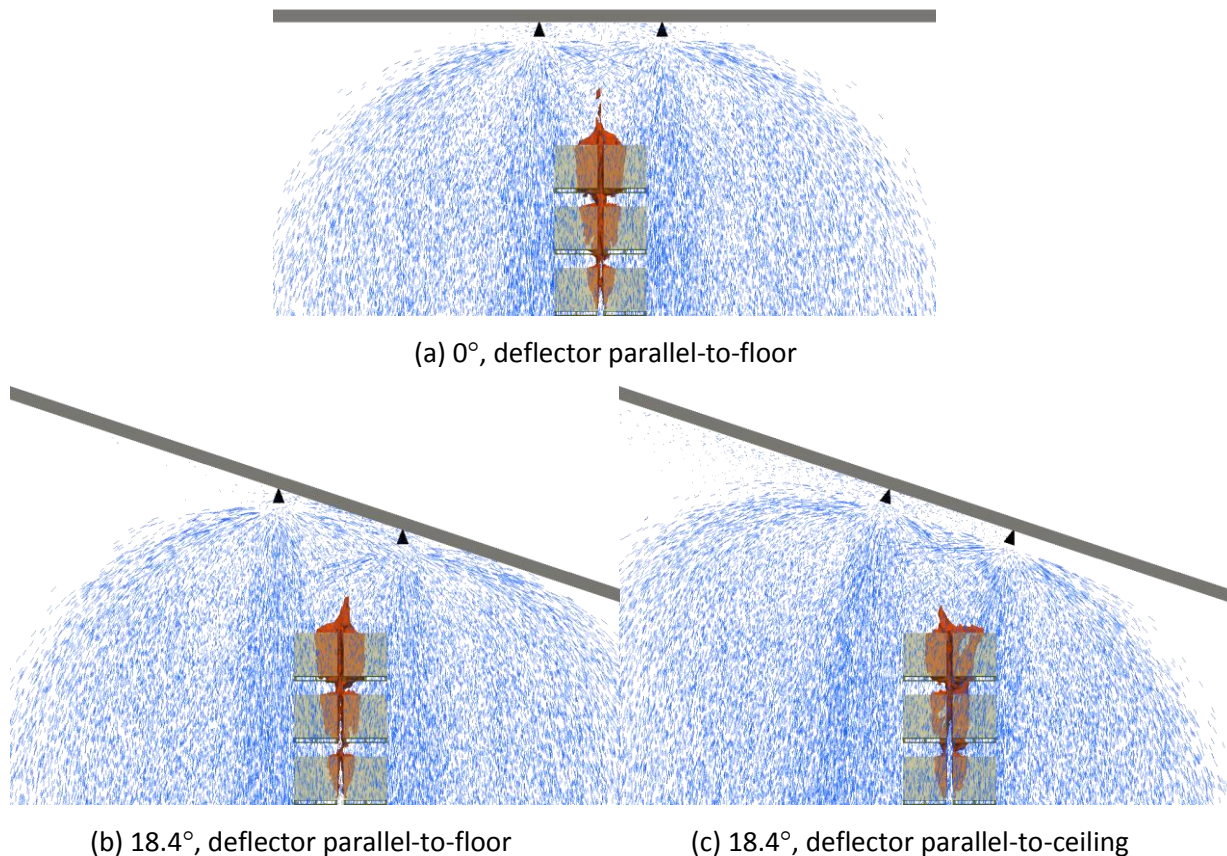


Figure 4-11: Instantaneous snapshots of sprays originating from four pendent K240 sprinklers (two injection locations are visible in the images) for (a) 0° inclination, deflector parallel-to-floor, (b) 18.4° inclination, deflector parallel-to-floor, and (c) 18.4° inclination, deflector parallel-to-ceiling. The 2.6-MW convective-HRR fire is shown by the instantaneous contour of the stoichiometric mixture fraction.

For the 0° inclination case, the maximum water flux occurs right below the pendent K240 sprinkler locations (see Figure 4-12(a)). Due to the presence of the 2.6-MW fire plume in the rack-storage region, the mass flux values observed are smaller ($<1 \text{ kg/m}^2\text{-s}$) compared to the regions below the sprinklers where values of $>2.3 \text{ kg/m}^2\text{-s}$ are observed.

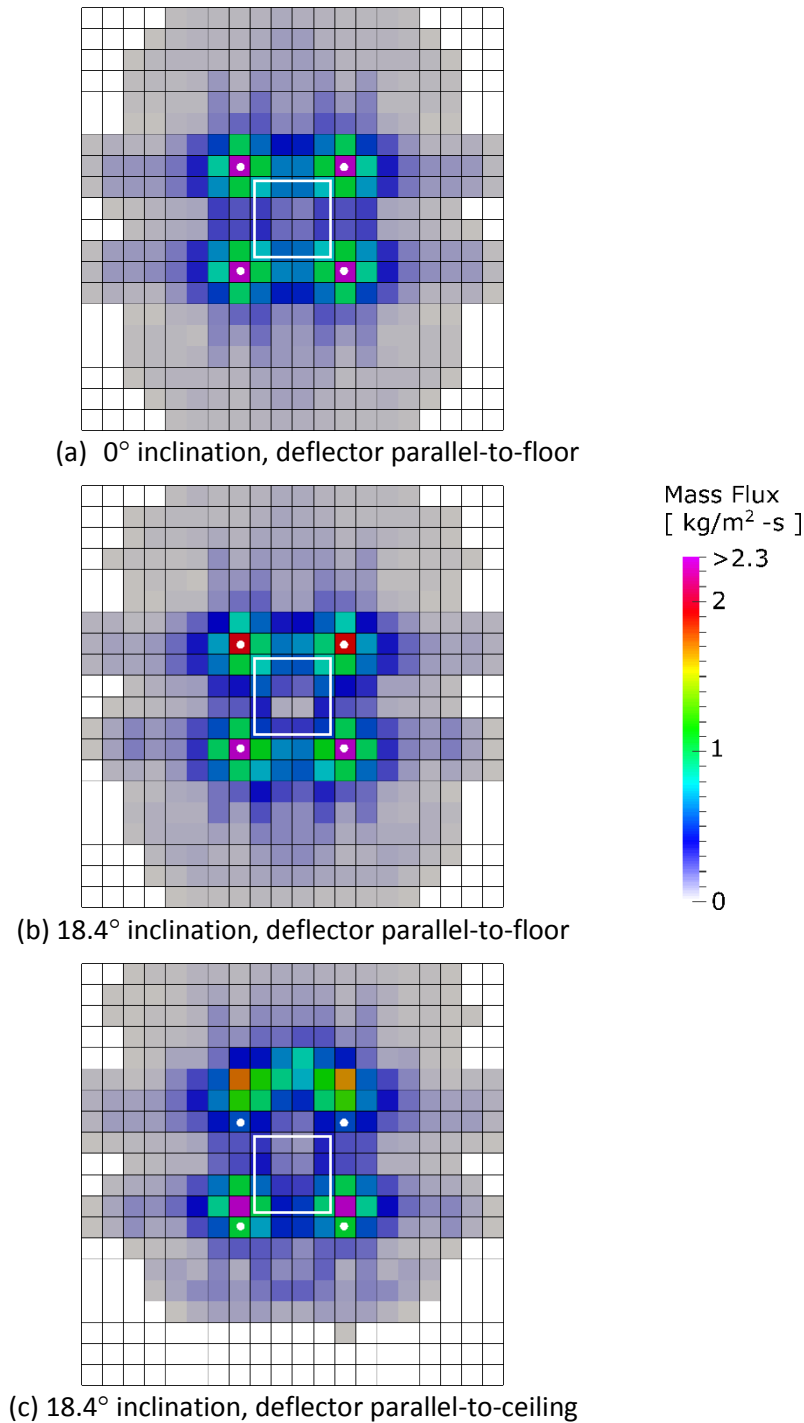


Figure 4-12: Comparison of droplet mass flux distributions shown for four pendent K240 sprinklers surrounding the ignition location when a 2.6-MW convective-HRR fire is present.

When the ceiling inclination is 18.4° and the sprinkler deflectors are parallel-to-floor, a higher mass flux below the sprinklers on the non-elevated side of the ceiling is observed than for the sprinklers on the elevated side ($\sim 2.3 \text{ kg/m}^2\text{-s}$ compared to $\sim 1.9 \text{ kg/m}^2\text{-s}$), as shown in Figure 4-12(b). The overall mass flux distribution is not affected as compared to the horizontal ceiling case. The relatively small difference of the distribution patterns between the horizontal and the 18.4° inclined ceiling cases with the deflectors parallel-to-floor was also observed for the pendent K200 sprinkler.

When the deflectors are kept parallel-to-ceiling, the water-flux distribution above the rack-storage array is shown in Figure 4-12(c). Compared to the distribution with deflectors parallel-to-floor, the peak mass flux occurs further away from the sprinkler location toward the elevated ceiling side. The maximum mass flux value on the elevated ceiling side is $\sim 1.7 \text{ kg/m}^2\text{-s}$. The overall distribution recorded shows similar trends as for the K200 sprinkler.

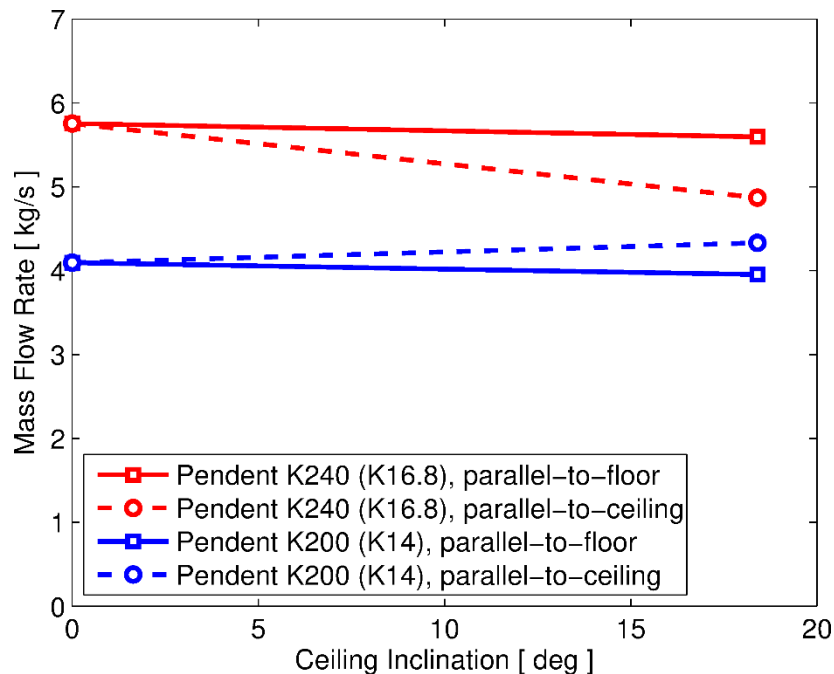


Figure 4-13: Time-averaged droplet mass flow rate through a $3.05 \text{ m} \times 3.05 \text{ m}$ ($10 \text{ ft} \times 10 \text{ ft}$) sampling area surrounding the ignition location at a height of 0.3 m (1 ft) above the CUP rack-storage array as a function of ceiling inclination. Four sprinklers are located below the ceilings with a fire of constant 2.6-MW convective HRR.

4.4.4 Comparison of Integrated Mass Flux

Integrated mass flow rates through a $3.05 \text{ m} \times 3.05 \text{ m}$ ($10 \text{ ft} \times 10 \text{ ft}$) area above the rack-storage array are also computed for the four sprinkler case. Figure 4-13 shows a comparison between mass flow rates for the K240 sprinkler at 2.4 bar (35 psi) and the K200 sprinkler at 3.4 bar (50 psi), when the 2.6-MW fire is present. When the ceiling is horizontal, compared to the K200 sprinkler mass flow rate, the K240 sprinklers provide $\sim 29\%$ higher mass flow rate over the $3.05 \text{ m} \times 3.05 \text{ m}$ ($10 \text{ ft} \times 10 \text{ ft}$) area. Inclining the ceiling at 18.4° and with the deflectors parallel-to-floor, the mass flow rate for both sprinklers remains

similar whereas, when the deflectors are parallel-to-ceiling, the K200 performance remains the same; however, the K240 flow rate decreases by ~15%. The differences between the K200 and K240 sprinkler designs (the deflector and orifice dimensions) affect the spray patterns, and thus affect the resulting mass flux distribution above the CUP. These discrepancies in sprinkler geometry can lead to different trends with ceiling inclination when the deflectors are kept parallel-to-ceiling.

4.5 Summary

The following observations can be made from the spray simulation results:

- For both the upright K160 and pendent K240 sprinklers, when the fire plume is not present, increasing the ceiling inclination from 0° to 18.4° causes a slight decrease in the water flux and the deflector orientation has negligible effect on the water-flux distribution.
- For one sprinkler directly above a 600-kW fire, the water-flux distribution from the upright K160 sprinkler is reduced significantly above the ignition location when the deflector is held parallel-to-ceiling. The same observation also holds true for the pendent K240 sprinkler.
- For the four sprinklers around the ignition location, in the presence of the 2.6-MW fire plume, the performance of the upright K160 sprinkler remains similar, irrespective of the deflector orientation. For the pendent K240 sprinkler, a small decrease in mass flow rate is observed when the deflector parallel-to-ceiling orientation is selected.

5. Conclusions and Recommendations

In the present study, simulations were conducted to determine sprinkler activation patterns and times under ceilings with obstructed construction (purlins, girders and ridges) for a range of ceiling slopes/inclinations. A growing fire on a 2 x 2 x 3 CUP rack-storage array with a maximum convective HRR of 15 MW was used as a plume source. Developing ceiling jets were presented and sprinkler activation calculations were made by decoupling activation from other suppression phenomena. Activation times and patterns for inclined ceilings were compared against horizontal ceiling results. Ceiling clearances of 3.05 m (10 ft) and 6.1 m (20 ft) to the ceiling midpoint were considered. Purlins of depths in the range of 0.1-0.6 m (4-24 in.), 0.6 m (24 in.) deep girders and ridges located 6.1-12.2 m (20-40 ft) from the ceiling midpoint were included in the simulations. Comparison was also made between quick-response, ordinary temperature (QR/OT) and standard-response, high temperature (SR/HT) sprinklers.

In addition, sprinkler spray simulations were conducted by selecting fixed fire source sizes for two scenarios: 1) when one sprinkler above the ignition location activates, and 2) when four sprinklers operate. In the case of four sprinklers, an average HRR was selected based on the sprinkler locations and predicted activation times. Sprays from two sprinklers, an upright K160 and a pendent K240, were simulated. Water-flux distributions were compared for various ceiling inclinations and sprinkler deflector orientations.

Ceiling inclination causes biased flow toward the elevated ceiling side due to buoyancy effect. However, the presence of purlins affects the upward flow pattern and tends to provide confinement of the combustion products. Results show that increasing purlin depth for a given ceiling inclination generally causes greater skewness of the activation pattern in the direction of the purlin channels.

From the range of conditions explored, major trends related to the most important parameters are summarized below and the following conclusions based on the trends can be drawn.

Activation in the absence of a ridge:

- Results from activation simulations involving QR/OT sprinklers show that, for horizontal ceilings (0°) and purlin depths of up to 0.6 m (24 in.), a marginal increase (maximum 4 s) in the average activation time is observed for the four sprinklers immediately adjacent to the fire source.
- For a ceiling inclination of 9.5° and purlin depths of up to 0.3 m (12 in.), the average activation time for the four sprinklers immediately adjacent to the fire source is similar to that of the case of horizontal ceilings for the same purlin depths. The average activation times are also comparable to those for the 9.5° smooth ceiling. For a purlin depth of 0.6 m (24 in.), considerable activation delay is observed for the non-elevated sprinklers. This delay may adversely impact suppression performance.
- For a ceiling inclination of 18.4° and purlin depths of up to 0.1 m (4 in.), the average activation time compares favorably with the smooth ceiling results. For the same slope and purlin depths

of 0.2 m (8 in.) and larger, considerable delays in non-elevated sprinkler activations are also observed which may affect suppression effectiveness.

- For SR/HT sprinklers, for ceilings 3.05 m (10 ft) above the CUP array and at inclination angles $\geq 9.5^\circ$ with a purlin depth of 0.3 m (12 in.), highly skewed activation patterns are observed between the elevated and non-elevated sides. As sprinklers on the non-elevated side do not activate, suppression effectiveness will be reduced.

Activation in the presence of a ridge:

- Presence of ridges marginally affects the activation times of the four sprinklers surrounding the ignition location. Activations near the ridge are also affected with slightly earlier activation times observed on the near side of the ridge. Reduced skewness of the sprinkler activation pattern toward the elevated side of the ceiling is also observed for reduced sprinkler stand-off distance.
- For an inclined ceiling at 18.4° with the ridge located 6.1 m (20 ft) from the CUP array, activation times near the ignition region are similar to those observed when the ridge is not present; however, significantly more SR/HT sprinklers activate near the ridge compared to an unbounded ceiling. The effect of the ceiling ridge on the sprinkler activation patterns appears more significant for SR/HT than for QR/OT sprinklers.

Sprinkler spray:

- From spray calculations for a single sprinkler above the ignition location when the fire plume is not present, for both the upright K160 and pendent K240 sprinklers, increasing the ceiling inclination from 0° to 18.4° causes a slight decrease in the water flux and the deflector orientation has negligible effect on the water-flux distribution.
- For one sprinkler directly above a 600-kW fire, the water-flux distribution from the upright K160 sprinkler is reduced significantly above the ignition location when the deflector is held parallel-to-ceiling. The same observation also holds true for the pendent K240 sprinkler.
- For the four sprinklers around the ignition location, in the presence of the 2.6-MW fire plume, the performance of the upright K160 sprinkler remains similar, irrespective of the deflector orientation. For the pendent K240 sprinkler, a small decrease in mass flow rate is observed when the deflector parallel-to-ceiling orientation is selected.

Based on the conclusions detailed above and from the Phase 1 study [1] a large-scale test plan can now be developed. The large-scale tests will provide validation of the simulation results. Test and modeling results will be used to update FM Global and NFPA standards [2] [12].

References

1. P. Chatterjee and K. V. Meredith, "Numerical Modeling of Sprinkler Activations and Spray Transport Under Sloped Ceilings," FM Global, Technical Report 2015.
2. "FM Global Data Sheet 2-0, Installation Guidelines for Automatic Sprinklers," FM Global, January 2014.
3. R. G. Bill Jr., H.-C. Kung, W. R. Brown, and E. E. Hill Jr., "Effects of Cathedral and Beamed Ceiling Construction on Residential Sprinkler Performance," *Fire Safety Science*, vol. 2, pp. 643-653, 1989.
4. W. D. Davis, G. P. Forney, and R. W. Bukowski, "International Fire Detection Research Project - Field Modeling: Simulating the Effect of Sloped Beamed Ceilings on Detector and Sprinkler Response," *Fire Protection Research Foundation Report*, 1994.
5. R. L. Vettori, "Effect of Beamed, Sloped, and Sloped Beamed Ceilings on the Activation Time of a Residential Sprinkler," National Institute of Standards and Technology, Gaithersburg, MD, Technical Report NISTIR 7079, 2003.
6. C. Mealy, J. Floyd, and D. Gottuk, "Smoke Detector Spacing Requirements Complex Beamed and Sloped Ceilings - Volume 1: Experimental Validation of Smoke Detector Spacing Requirements," *Fire Protection Research Foundation Report*, 2008.
7. FireFOAM. [Online]. <http://www.fmglobal.com/modeling>
8. Y. Wang, P. Chatterjee, and J. L. de Ris, "Large Eddy Simulation of Fire Plumes," *Proceedings of the Combustion Institute*, vol. 33, no. 2, pp. 2473-2480, 2011.
9. Fire and Risk Alliance. [Online]. <http://www.fireriskalliance.com>
10. K. E. Isman, S. J. Jordan, A. W. Marshall, and N. L. Ryder, "Research Plan for Sloped Ceiling Storage Protection," *Fire Protection Research Foundation Report*, November 2015.
11. X. Zhou, S. P. D'Aniello, and H.-Z. Yu, "Spray Characterization Measurements of a Pendent Fire Sprinkler," *Fire Safety Journal*, vol. 54, pp. 36-48, 2012.
12. "NFPA 13: Standard for the Installation of Sprinkler Systems," National Fire Protection Association, 2016.
13. "OpenFOAM: The Open Source CFD Toolbox, User Guide, Version 2.2.0," February 22, 2013.

14. OpenFOAM v3 User Guide: 5.4 Mesh generation with snappyHexMesh. [Online].
<https://cfd.direct/openfoam/user-guide/v3-snappyHexMesh>
15. J. Floyd, E. Budnick, M. Boosinger, J. Dinaburg, and H. Boehmer, "Analysis of the Performance of Residential Sprinkler Systems with Sloped or Sloped and Beamed Ceilings," *Fire Protection Research Foundation Report*, July 2010.
16. E. Carlsson, "Comparison of Sprinkler Activation in Flat and Sloping Ceilings using FDS 6," Lund University, Report 5404, 2013.
17. G. Agarwal, A. Gupta, M. Chaos, K. V. Meredith, and Y. Wang, "An Experimental and Modeling Approach to Investigate the Burning Behavior of Cartoned Unexpanded Plastic Commodity," in *9th U.S. National Combustion Meeting*, Cincinnati, OH, 2015.
18. P. Chatterjee, J. L. de Ris, Y. Wang, and S. B. Dorofeev, "A Model for Soot Radiation in Buoyant Diffusion Flames," *Proceedings of the Combustion Institute*, vol. 33, no. 2, pp. 2665–2671, 2011.
19. P. Chatterjee, K. V. Meredith, and Y. Wang, "Temperature and Velocity Distributions from Numerical Simulations of Ceiling Jets Under Unconfined, Inclined Ceilings," *Fire Safety Journal*, vol. 91, pp. 461-470, 2017.
20. P. Chatterjee, K. V. Meredith, B. Ditch, H.-Z. Yu, Y. Wang, and F. Tamanini, "Numerical Simulations of Strong-Plume Driven Ceiling Flows," *Fire Safety Science*, vol. 11, pp. 458-471, 2014.
21. Y. Wang, K. V. Meredith, X. Zhou, P. Chatterjee, Y. Xin, M. Chaos, N. Ren, and S. B. Dorofeev, "Numerical Simulation of Sprinkler Suppression of Rack Storage Fires," *Fire Safety Science*, vol. 11, pp. 1170-1183, 2014.
22. K. V. Meredith, P. Chatterjee, X. Zhou, Y. Wang, and H.-Z. Yu, "Validation of Spray Water Distribution Patterns for the K11.2 Sprinkler in the Presence of a Rack Storage Fire Plume Generator," *Proceedings of the 13th Fire Science and Engineering Conference (INTERFLAM)*, pp. 307-316, 2013.
23. K. V. Meredith, P. Chatterjee, Y. Wang, and Y. Xin, "Simulating Sprinkler Based Rack Storage Fire Suppression under Uniform Water Distribution," *Proceedings of the Seventh International Seminar on Fire & Explosion Hazards*, pp. 511-520, 2013.
24. A. Gupta, K. V. Meredith, G. Agarwal, S. Thumuluru, Y. Xin, M. Chaos, and Y. Wang, "Development of a CFD Model for Large-Scale Rack-Storage Fires of Cartoned Unexpanded Plastic Commodity," in *2nd European Symposium of Fire Safety Science*, Nicosia, Cyprus, 2015.



Printed in USA © 2017 FM Global
All rights reserved.
fmglobal.com/researchreports

FM Insurance Company Limited
1 Windsor Dials, Windsor, Berkshire, SL4 1RS
Authorized by the Prudential Regulation Authority and regulated by the Financial Conduct
Authority and the Prudential Regulation Authority.